Osteological Correlates of Cephalic Skin Structures in Amniota: Documenting the Evolution of Display and Feeding Structures with Fossil Data

A dissertation presented to

the faculty of

the College of Arts and Sciences of Ohio University

In partial fulfillment

of the requirements for the degree

Doctor of Philosophy

Tobin L. Hieronymus

March 2009

© 2009 Tobin L. Hieronymus. All Rights Reserved.

This dissertation titled

Osteological Correlates of Cephalic Skin Structures in Amniota: Documenting the Evolution of Display and Feeding Structures with Fossil Data

by

TOBIN L. HIERONYMUS

has been approved for

the Department of Biological Sciences

and the College of Arts and Sciences by

Lawrence M. Witmer

Chang Ying-Chien Professor of Paleontology

Benjamin M. Ogles

Dean, College of Arts and Sciences

ABSTRACT

HIERONYMUS, TOBIN L., Ph.D., March 2009, Biological Sciences

Osteological Correlates of Cephalic Skin Structures in Amniota: Documenting the Evolution of Display and Feeding Structures with Fossil Data (254 pp.)

Director of Dissertation: Lawrence M. Witmer

The research presented here is an examination of the morphology and histology of several broad categories of skin structures in living amniotes, together with analyses of the osteological correlates associated with each skin category. The epidermal horn and armor-like dermis of extant rhinoceros are examined in detail, and the evolution of both of these skin structures is reconstructed in phylogenetic context from fossil evidence. The evolution of rhinoceros dermal armor is strongly associated with the evolution of shearing tusks used in fighting behaviors, and precedes the evolution of epidermal horns by ~20 Ma. The distribution and morphology of cephalic scales, rhamphothecal plates, and feathers in Sauropsida is then examined in an analysis of evolutionary modularity. Two distinct regions of skin, one around the mouth and another on the skull roof, show independent patterns of morphological evolution, suggesting that skin features in these regions are interconnected as modules. Rhamphotheca in neornithine birds are one possible expression of this modularity. In a separate analysis, plates of compound rhamphotheca (e.g., in albatross) are shown to be homologous with regions of simple rhamphotheca. Rhamphotheca occupy a topographically similar area of skin in nearly all neornithine birds, and the variable expression of softer grooves leads to several homoplastic occurrences of compound rhamphotheca. Several adaptive scenarios have

been proposed for novel skin structures in non-avian dinosaurs, but the lack of direct fossil evidence for skin in these animals and the ambiguity in available reconstructions has made it difficult to evaluate these scenarios. Detailed reconstructions for cephalic skin structures drawing on gross morphology and paleohistology are presented for the lineage of centrosaurine dinosaurs leading to *Pachyrhinosaurus* and for the abelisaurid theropod *Majungasaurus*. The transition from tall horn cores to gnarled pachyostotic bosses in centrosaurine dinosaurs closely resembles the morphology and evolution of the frontal boss in muskox. The rugose bone on *Majungasaurus* skulls closely resembles the attachment of dermal armor in rhinoceros. In both cases, agonistic behaviors associated with similar skin structures in extant animals cast doubt on the idea that they functioned only in visual display. The evolution of these novel structures was most likely driven by social selection.

Approved: _____

Lawrence M. Witmer

Chang Ying-Chien Professor of Paleontology

DEDICATION

This work is dedicated to my mother,

Barbara Lee Hieronymus

Because of all the outstanding teachers I have had, she was the first,

from my place in her preschool class to the present day, to show me how learning comes

alive when the connections between people are genuine and attentive;

and to my father,

Fred Randall Hieronymus

because much of my childhood reads like a chapter from Between Pacific Tides*;*

I now understand how beautiful a gift it was as to learn with him, and also how precious

it was for him to teach me, as I hope to teach others in turn.

ACKNOWLEDGMENTS

Discussion and correspondence with Lorenzo Alibardi, Audrone Biknevicius, Lisa Noelle Cooper, Philip Currie, Joseph Daniel, David Dufeau, Andew Farke, Cynthia Marshall Faux, Mark Goodwin, Sue Herring, Robert Hill, Casey Holliday, Dominique Homberger, Angela Horner, Jack Horner, John Hutchinson, Andrew Lee, Gerald Mayer, Eric McElroy, Hillary Maddin, Paul Maderson, Matt Milbachler, Donald Miles, Molly Morris, Patrick O'Connor, Chris Organ, Kevin Padian, Erin Rasmusson, Steve Reilly, Margaret Rubega, Michael Ryan, Natalia Rybczinski, Torsten Scheyer, Nancy Stevens, Alycia Stigall, Darren Tanke, Takanobu Tsuihiji, Matt Vickaryous, Susan Williams, and Larry Witmer have all greatly aided this research. For access to histology and microscopy equipment I wish to thank Dan Hembree, David Kidder, Greg Nadon, Patrick O'Connor, Gar Rothwell, and Susan Williams. David Dufeau and Ryan Ridgely at OUμCT provided invaluable assistance with CT scanning. For access to osteological and paleontological specimens, I wish to thank James Gardner at the Royal Tyrrell Museum; Jack Horner, Pat Lieggi, Carrie Ancell, Bob Harmon, David Varrichio, Ellen-Thérèse Lamm, and Susan Winking at the Museum of the Rockies; Kevin Seymour and Mark Peck at the Royal Ontario Museum; Greg Schneider and Janet Hinshaw at the University of Michigan Museum of Zoology; Mark Goodwin, Pat Holroyd, and Kevin Padian at the University of California Museum of Paleontology; Steve Rogers and Suzanne Mclaren at the Carnegie Museum of Natural History; Linda Gordon, Robert Purdy, and Matt Carrano at the National Museum of Natural History; Eileen Westwig, Paul Sweet, Susan Bell, Carl Mehling, and Mark Norell at the American Museum of Natural History; Christine

Lefèvre and Alexis Martin at the Muséum national d'Histoire naturelle; Gerald Mayer at the Naturmuseum Senckenberg; Link Olson at the University of Alaska Museum; and Scott Sampson, Mike Getty, Mark Loewen, and Eric Lund at the University of Utah Museum of Paleontology. This research was funded by the Jurassic Foundation (TLH), the National Science Foundation (NSF IBN-0343744 & IOB-0517257; LMW), and Ohio University (TLH).

TABLE OF CONTENTS

Page

LIST OF TABLES

Page

LIST OF FIGURES

Page

CHAPTER 1: THE STRUCTURE OF WHITE RHINOCEROS (*CERATOTHERIUM SIMUM*) HORN INVESTIGATED BY X-RAY COMPUTED TOMOGRAPHY AND HISTOLOGY WITH IMPLICATIONS FOR GROWTH AND EXTERNAL FORM

Abstract

The nasal and frontal horns of two individuals of *Ceratotherium simum* were examined by x-ray computed tomography (CT scanning), gross observation of sectioned horn, and light microscopy of histological sections of the horn tissue. CT scans of both sets of horns reveal a periodic banding pattern that is evident upon gross observation of sections as darker bands of tissue. The overlap of these bands in both histological and CT slices suggests the presence of both a photoabsorbent component (melanin) and a radiodense component (calcium phosphate salts, most likely hydroxyapatite or octocalcium phosphate). The distribution of these two components in the horns is hypothesized to contribute to the differential wear patterns that produce the characteristic sweeping conical shape of rhinoceros horn from what otherwise (in the absence of wear and UV exposure) would be cylindrical blocks of constantly growing cornified papillary epidermis. Although extant rhinocerotids are unique in possessing a massive entirely keratinous horn that approximates the functions of keratin-and-bone horns such as those of bovid artiodactyls, the tissue structures that make up the horn are strikingly convergent with other examples of papillary cornified epidermis found in horses, artiodactyls, cetaceans, and birds.

Introduction

Rhinoceros horns are unusual among the horns of ungulates in that they lack a bony horn core. Instead, the horns are anchored to the dermis covering the frontal and nasal bones, and are associated with pronounced bony rugosities in most individuals (Hieronymus and Witmer, 2004). The true 'horny' part of rhinoceros horn is an epidermal derivative, consisting of keratinized tubules of cells set in an amorphous keratinized matrix. The tubules comprise approximately 40 lamellae of squamous cells and range from 300 to 500 μm in diameter (Ryder, 1962). The amorphous matrix is made up of keratinized fusiform interstitial cells (Lynch, 1973). Each tubule grows from a generative layer of epidermis (stratum germinativum) covering a dermal papilla. The amorphous matrix is grown from the stratum germinativum of the epidermis between dermal papillae. As the epithelial cells of the horn are dead upon the completion of keratinization, all growth in rhinoceros horn takes place at the base.

Rhinoceros horns, as structures formed of cornified papillary epidermis, are part of a phylogenetically diverse assemblage of convergent cornified epidermal appendages, including the cornified sheaths of pecoran artiodactyl horns, bird beaks, turtle beaks, amniote claws and hooves, and baleen (Homberger, 2001). The independent origin of each of these examples provides a basis for identifying convergent morphologies, which in turn may shed light on functional aspects of cornified papillary epidermis (e.g., resistance of tubules to bending, preferential tearing directions). Here we report on previously undescribed aspects of melanization and calcification in the horns of white

rhinoceros *Ceratotherium simum*, and discuss the impact these that features may have on the growth and shape of the horn.

Materials and Methods

The horns examined in this study came from two individuals, a 32-year-old female (Ohio University Vertebrate Collection [OUVC] 9541) formerly housed at The Wilds (Cumberland, Ohio) and a 41-year-old male (OUVC 9754) formerly housed at the Phoenix Zoo (Phoenix, Arizona). Both animals died for reasons unrelated to this study.

The nasal and frontal horns of OUVC 9541 (Fig. 1-1A) and the frontal horn of OUVC 9754 were bisected in the midsagittal plane for gross anatomical observation. A longwave ultraviolet lamp (Ultra Violet Products UVL-26P, Upland) was used to examine fluorescence in the epidermal horn (Fig. 1-1A). The right half of the nasal horn of OUVC 9541 and the entire frontal horn of OUVC 9754 were scanned on a GE HiSpeed FX/i Helical CT scanner at O'Bleness Memorial Hospital in Athens, Ohio. Slice thickness and spacing was 1mm. Scanning parameters for OUVC 9541 were 120kV and 150mA, whereas those for OUVC 9754 were 120kV and 120mA. Field of reconstruction was 278mm for OUVC 9541 and 282mm for OUVC 9754 for 512 x 512 pixels using a bone algorithm. CT data were compiled in the Amira 3.1.1 (Mercury-TGS, San Diego) and eFilm 2.0 (Merge-eFilm, Toronto) software packages for analysis and three-dimensional reconstruction.

Portions along a medial parasagittal section of the horn of OUVC 9541 (Fig. 1-1A) were embedded in EpoThin epoxy (Buehler, Lake Bluff), mounted on plastic slides, and ground to approximately 2 mm thickness. This set of unstained sections was

examined by transmitted light microscopy to determine melanin distribution within the horn.

Results

Horn is deposited dorsoventrally in successive sheets (here termed horn laminae) with irregular layers of approximately 1.0 – 2.0 mm. Each lamina represents a presumably coeval period of growth of horn tubules and intertubular matrix. In sagittal or transverse section, horn laminae appear as bands (Fig. 1-1B, C). The horn laminae fluoresce under UV light, aiding in their delineation. The color value of each lamina varies across its lateral extent, such that the central part of each lamina is darker in color than the periphery. This central dark patch is not uniform along the length of the horn, but rather shows pulses of darker horn interspersed with lighter horn. These dark patches alternate at an approximately 6 cm interval (Fig. 1-1A). The pattern of dark patches is also visible in CT as alternating radiolucent and radiodense bands (Fig. 1-1D). Gross examination of the frontal horn shows a similar pattern of periodic dark patches, at an approximately 2 cm interval (Fig. 1-1A), and horn laminae that alternate irregularly at approximately 0.5 – 2.0 mm (Fig. 1-1B).

Histological examination of thick sections shows that within dark patches, more heavily pigmented cornified epidermal tissue is restricted to the intertubular matrix (Fig. 1-2). The horn tubules themselves retain a similar light color from the edge of the horn to its center. Rhinoceros horn can thus be viewed as a composite material, with tubules of keratinocytes forming 'fibers' that are embedded in a matrix of varying composition (Fig. 1-3).

Discussion

Periodic banding and annual growth

The 6 cm periodicity of the radiodense dark patches in the nasal horn corresponds very well with annual growth rates of white rhinoceros nasal horn in wild populations (~5 cm/yr per Pienaar et al., 1991; 5–6 cm/yr per Rachlow and Berger, 1997; both rates were measured from internal landmarks in the horns and represent tissue turnover rather than whole-horn elongation). The 2 cm periodicity of the frontal horn reflects its relatively slower growth, which is also consistent with the findings of Rachlow and Berger (1997). The periodicity of the horn laminae is much more irregular. Color value changes between adjacent horn laminae may be more akin to fault bars in feathers, which are caused by changes in keratinization due to external factors (mechanical damage, diet, etc.) during feather growth (Prum and Williamson, 2001).

Seasonal variation in the growth rates of other keratinized tissues such as the claws of sheep and cattle have been variously linked to changes in photoperiod and changes in temperature (Clark and Rakes, 1982; Hahn et al., 1986). OUVC 9541 spent the entirety of its life outside of the climate and historical latitudinal range of naturally occurring white rhinoceros populations (~40° N in Ohio, U.S.A., compared to a probable historical range in Africa of ~33° N to 33° S as per Groves, 1972). OUVC 9754, however, lived in an environment (Arizona, U.S.A.) that is quite similar to the northern- and southern-most extent of the African range. As both of these specimens show similar periodic structures in their horns, we are confident that this horn morphology is not simply an artifact of unusual environments.

Co-occurrence of radiodense features and dark periodic bands

The intensity of the dark patches suggests that there are differences in the rate of melanin deposition during the process of horn growth. Although this satisfactorily explains the gross observation results, melanin itself is not radiodense enough to produce similar patterns in a radiograph. The difference in contrast in radiography can be attributed to higher concentrations of calcium salts accompanying melanin deposition in the dark patches. Co-occurrence of melanin and calcium (as octocalcium phosphate) has been noted in the horns of saiga (*Saiga tatarica*) (Hashiguchi et al., 2001). The presence of higher concentrations of calcium can be interpreted as a primary mechanism and not a pathological finding, as several other forms of horny tissue aside from rhino and saiga horn also contain appreciable portions of hydroxyapatite or octocalcium phosphate (Arnott and Pautard, 1968; Pautard, 1970; Hashiguchi et al., 1995).

Horn growth and shape

The generalities of rhinoceros horn morphology have been fairly well understood for quite some time (Boas, 1931), but the mechanism by which horns maintain this morphology has received little attention. The variations in melanin content and calcification described here provide a mechanistic basis for controlling horn shape by differential wear.

Melanin has been variously implicated in increasing the hardness and strength (Bonser and Witter, 1993; Bonser, 1996b) as well as the long term resistance to wear (Averill, 1923; Bonser, 1996a) of cornified epidermal structures at a gross level. However, a number of studies have shown no quantifiable increase in work-to-fracture or

hardness (stiffness) associated with melanin in cornified epidermal tissues such as horse hoof wall and feather barb (Bertram and Gosline, 1986; Douglas et al., 1996; Butler and Johnson, 2004), thus refuting a mechanically significant role for melanin in these systems. However, keratins are substantially weakened by prolonged exposure to UV light (Marshall, 1986), and melanin may act to reduce the degree of wear by absorbing light entering the tissue (Jimbow et al., 1986). Although melanin itself does not appear to contribute to increased work-to-fracture or hardness, it is highly probable that calcification accompanying melanization (as shown by Hashiguchi et al. [2001] and this study) changes the hardness or compressional modulus of these tissues. The co-occurrence of calcification in melanized cornified epidermis may be responsible for the equation of hardness and melanization reported in other systems (Bonser and Witter, 1993; Bonser, 1996a).

The higher concentration of melanin and calcium salts in the center of white rhinoceros horn is likely to play a role in determining the overall conical shape of the horn. Healthy horn grows at a nearly constant rate throughout its areal extent. In the absence of any wear or keratin degradation, growing rhinoceros horn would form a gently curving cylinder. Three major factors combine to remove material from the horns by abrasion and wear: (1) UV-induced keratin degradation (Marshall, 1986); (2) reduced work-to-fracture as the horn tissue desiccates (Bertram and Gosline, 1987; Kitchener, 1987); and perhaps most importantly (3) stereotypical behavioral use patterns, such as scraping and 'horn-wiping' on the ground, vegetation, or bars in an enclosure, and horn-clashing between individuals (Bigalke, 1946; Kingdon, 1979; Owen-Smith, 1988;

Dinerstein, 2003). Progressive wear on older (i.e., more distal, dehydrated, and UV-damaged) portions of the horn produces the characteristic conical horn shape. The fact that mature males engage in more frequent bouts of scraping and horn-clashing than females may thus explain their slightly shorter horns (Kingdon, 1979).

The horns of many rhinos are not uniformly conical, but rather show a marked change in slope, such that the base forms a squat cone and the distal part continues as a more tapered cone. This change reflects the rate at which softer outer horn is worn away to expose more resistant material in the center. The change occurs near the point where the more heavily melanized and calcified tissue nears the external wear surface (arrow in Fig. 1-1A). The difference between the concentration of melanin and calcium salts in the intertubular matrix of the horn and the tubules themselves suggests that the intertubular matrix is responsible for these differences in hardness.

Conclusions

Rhinoceros horn provides an independently derived example of a cornified papillary epidermal appendage. The concentration of melanin and calcium salts in the core of rhinoceros horn varies annually, and appears to play a role in maintaining characteristic horn morphology. Local differences in melanin content and calcium salts reflect changes in the composition of the intertubular matrix, without necessarily involving the tubules of the papillary dermis.

Although the specific disposition of melanin and calcium salts in rhinoceros horn is perhaps unique among cornified papillary epidermis, the general tissue structure that forms rhinoceros horn is strongly convergent with many similar tissues, such as ungulate

hoof wall (Nickel, 1938), bovid artiodactyl horns (Trautmann and Fiebiger, 1952:368), baleen plates (Lambertsen et al., 1989), and the papillary horn of cockatoo bills (Homberger, 2001). Comparative studies that take advantage of this convergence may shed light on phylogenetic and functional controls on cornified epidermis morphology.

Literature Cited

Arnott HJ, Pautard FGE. 1968. The inorganic phase of bone: A re-appraisal. Calcified Tissue Reseach 2(suppl.):2.

Averill CK. 1923. Black wing tips. Condor 25:57–59.

Boas, JEV. 1931. In: Bolk L, Göppert E, Kallius E, Lubosch W, editors. Handbuch der Vergleichenden Anatomie der Wirbeltiere.

Bertram JEA, Gosline JM. 1986. Fracture toughness design in horse hoof keratin. Journal of Experimental Biology 125:29–47.

Bertram JEA, Gosline JM. 1987. Functional design of horse hoof keratin: the modulation of mechanical properties through hydration effects. Journal of Experimental Biology 130:121–136.

Bigalke R. 1946. The regeneration of the anterior horn of the black rhinoceros, *Diceros bicornis* (Linn.). Proceedings of the Zoological Society of London 115:323–326.

Bonser RHC. 1996a. Comparative mechanics of bill, claw, and feather keratin in the Common Starling, *Sturnus vulgaris*. Journal of Avian Biology 27: 175–177.

Bonser RHC. 1996b. The mechanical properties of feather keratin. Journal of Zoology (London) 239: 477–484.

Bonser RHC, Witter MS. 1993. Indentation hardness of the bill keratin of the European Starling. Condor 95: 736–738.

Butler M, Johnson A. 2004. Are melanized feather barbs stronger? Journal of Experimental Biology 207:285–293.

Clark AK, Rakes AH. 1982. Effects of methionine hydroxy analog supplementation on dairy cattle hoof growth and composition. Journal of Dairy Science 65:1439–1502.

Dinerstein E. 2003. The return of the unicorns: the natural history and conservation of the greater one-horned rhinoceros. New York: Columbia University Press.

Douglas JE, Mittal C, Thomason JJ, Jofriet JC. 1996. The modulus of elasticity of equine hoof wall: Implications for the mechanical function of the hoof. Journal of Experimental Biology 199:1829–1836.

Groves CP. 1972. *Ceratotherium simum*. Mammal Species 8:1–6.

Hahn MV, McDaniel BT, Wilk JC. 1986. Rates of hoof growth and wear in Holstein cattle. Journal of Dairy Science 69:2148–2156.

Hashiguchi K, Hashimoto K. 1995. The mineralization of crystalline inorganic components in Japanese serow horn. Okajimas Folia Anatomica Japan 72:235–244.

Hashiguchi K, Hashimoto K, Akao M. 2001. Morphological character of crystalline components present in saiga horn. Okajimas Folia Anatomica Japan 78:43–48.

Hieronymus TL, Witmer LM. 2004. Rhinoceros horn attachment: Anatomy and histology of a dermally influenced bone rugosity. Journal of Morphology 260:298.

Homberger DG. 2001. The case of the cockatoo bill, horse hoof, rhinoceros horn, whale baleen, and turkey beard: The integument as a model system to explore the concepts of homology and non-homology. In: Dutta HM, Datta Munshi JS, editors. Vertebrate functional morphology: Horizon of research in the 21st century. Enfield: Science Publishers Inc. p 317-343.

Jimbow K, Fitzpatrick TB, Quevedo WC Jr. 1986. Formation, chemical composition and function of melanin pigments. In: Bereiter-Hahn J, Matoltsy AG, Sylvia Richards K, editors. Biology of the integument, vol. 2: Vertebrates. Berlin: Springer. p 278–292.

Kingdon J. 1979. East African mammals, vol IIIB. Chicago: University of Chicago Press. 436 p.

Kitchener A. 1987. Fracture toughness of horns and a reinterpretation of the horning behaviour of bovids. Journal of Zooloy (London) 213:621–639.

Lambertsen RH, Hintz RJ, Lancaster WC, Hirons A, Kreiton KJ, Moor C. 1989. Characterization of the functional morphology of the mouth of the Bowhead Whale, *Balaena mysticetus*, with special emphasis on feeding and filtration mechanisms. Report to the Department of Wildlife Management, North Slope Borough, Box 69, Barrow, AK from Ecosystems, Inc., Institute for Environmental Medicine, University of Pennsylvania Medical Center, Philadelphia, PA 19104. 134 pp.

Lynch LJ, Robinson V, Anderson CA. 1973. A scanning electron microscope study of the morphology of rhinoceros horn. Australian Journal of Biological Sciences 26:395–399.

Marshall RC. 1986. Nail, claw, hoof, and horn keratin. In: Bereiter-Hahn J, Matoltsy AG, Richards SK, editors. Biology of the integument, vol. 2: Vertebrates. Berlin: Springer. p 722–738.

Nickel R. 1938. Uber den Bau der Hufrorchen und seine Bedeutung fur den Mechanismus des Pferdhufes. Deutsche Tierarztliche Wochenschrifte (Hannover) 46:449–552.

Owen-Smith RN. 1988. Megaherbivores. Cambridge: Cambridge University Press. 369 p.

Pautard FGE. 1970. The mineral phase of calcified cartilage, bone, and baleen. Calc Tiss Res 4(suppl.):34–36.

Pienaar DJ, Hall-Martin AJ, Hitchins PM. 1991. Horn growth rates of free-ranging white and black rhinoceros. Koedoe 34:97–105.

Prum RO, Williamson S. 2001. Theory of the growth and evolution of feather shape. Journal of Experimental Zoology 291:30–57.

Rachlow JL, Berger J. 1997. Conservation implications of patterns of horn regeneration in dehorned white rhinos. Conservation Biology 11:84–91.

Ryder ML. 1962. Structure of rhinoceros horn. Nature 193:1199–1201.

Trautmann A, Fiebiger J. 1952. Fundamentals of the histology of domestic animals. Ithaca: Comstock Publishing Associates. 426 p.

CHAPTER 2: ADAPTATION, EXAPTATION, AND CONVERGENCE IN RHINOCEROTID HORN EVOLUTION

Abstract

All living rhinoceros possess both (a) elaboration of the dermis as body armor and (b) derived dermal support of their characteristic epidermal horns. Here we show that two separate bony indicators for these traits can be seen in fossil taxa, revealing two independent evolutionary events leading to the appearance of rhinoceros horns. Rhinoceros dermal armor first appeared in the late Eocene (39–42 Ma) as an adaptive response to the use of shearing tusks in intraspecific agonistic behavior. The stiff collagenous tissue of dermal armor was then exapted to support solid epidermal horns in the early Miocene (16–20 Ma). The separation of these two events suggests that rhinoceros horns did not arise as a single novel adaptation, but rather as a sequence of discrete responses to different selection regimes.

Introduction

Rhinoceros horn evolution has acquired iconic status as an example of evolutionary novelty and adaptation (Lewontin 1978; Coddington 1990), but the adaptive explanations and evolutionary scenarios proposed for the appearance of rhinoceros horns have proved to be more problematic than similar events in other taxa, such as horn and antler evolution in artiodactyls. Like other ungulate horns, rhinoceros horns have been hypothesized to function as organs of antipredator defense (Lewontin 1978) or intraspecific display (Berger and Cunningham 1998; Rachlow et al. 1998). Whereas most amniote horns are composed of a thin keratin sheath covering a large bony process,

rhinoceros horn is a unique arrangement of massive epidermal tissue (Ryder 1962) lacking a bony core and supported only by dense dermis (Fig. 2-1). This dense and highly organized structure, in fact, characterizes the dermis across most of the body, and appears to function as dermal armor (Shadwick et l. 1992), particularly in the neck and flanks. Similar arrangements of dermis have arisen independently in such distantly related mammals as hippopotamids, suids, hyrax, and pinnipeds (Schumacher 1931; Sokolov 1982).

Existing reconstructions of extinct rhinocerotids typically point to any form of rugosity on the nasal bones as evidence of horns (Cerdeño 1995; Antoine 2002). Moreover, a typological conception of rhinoceros (the name literally means ‘nose horn’) has no doubt also played some role, to the point of nasal horn reconstructions made even in the absence of any attachment rugosity. Such broadly defined interpretations place the first occurrence of horns at *Diceratherium* in the latest early Oligocene at approximately 30 Ma, and portray most subsequent rhinocerotids as horned.

Examining the evolutionary history of these soft-tissue features requires an assessment of the causal relationship between skin morphology and any bony elements that may be preserved in fossil taxa. By studying extant taxa with similar skin morphologies, the osteological correlates or bony signatures of specific skin attributes can be directly established, and fossil taxa can then be surveyed for more informative bony indicators. Distinguishing the bony indicators of dermal armor from those of horns in extant rhinocerotids allows a reassessment of the evolutionary history of these skin-related characters in extinct taxa.

Results & Discussion

Osteological correlates of dermal armor

In extant rhinoceros, the presence of dermal armor on the skull is marked by several patches of rugose bone (Fig. 2-2C). This rugose surface is the result of the direct formation of bone from dermal tissue (metaplastic ossification; Fig. 2-2B). Similar patches of rugose bone are also found on skulls of hippopotamus (Fig. 2-3) and the African suids *Hylochoerus* and *Potamochoerus*, all of which are hornless, suggesting that rugosity alone is not a sufficient signature of horn attachment in extinct rhinocerotids.

Osteological correlates of integumentary horns

Ossification features associated with horns can be distinguished from those associated only with dermal armor by the presence of an annular (ring-shaped) distribution of rugose bone (Fig. 2-2A), presumably the result of epigenetically-controlled bone growth in response to stress concentrations at the edges of heavily keratinized horns. Similar patterns, albeit at a much smaller scale, can be seen in other taxa with prominent rigid skin appendages, such as the comb duck *Sarkidiornis* and the American white pelican *Pelecanus erythrorhynchos* (Fig. 2-4). This distinction allows two separate skin-related characters to be scored for fossil taxa: (a) presence or absence of homogeneous patches of rugose bone (the bony signature for dermal armor), and (b) presence or absence of annular rugosities (the signature for epidermal horns).

Osteological correlates of dermal armor in fossil taxa

Homogeneous patches of rugose bone on other regions of the skull appear more basally than nasal rugosities, with faint expression on the squamosal bones of *Trigonias*

osborni (39–42 Ma) and well-developed squamosal rugosity in *Subhyracodon* spp. (Fig. 2-5). Squamosal rugosity (Fig. 2-3D) is in fact the most widespread evidence of dermal armor in extinct rhinocerotids, and is the most pronounced cranial rugosity in the elasmotherine lineage (Deng 2005; *Diceratherium – Huaqintherium* in Fig. 2-5), even persisting after nasal rugosities have been secondarily lost in more derived taxa such as *Procoelodonta*.

Osteological correlates of epidermal horns in fossil taxa

The nasal rugosities of basal rhinocerotids such as *Diceratherium* and *Menoceras* do not form annular patterns (Figs. 2-6 & 2-7), and thus do not provide any positive evidence for the presence of horns. In fact, we found such evidence only in the crown group of living rhinocerotids, which includes the extinct taxa *Coelodonta* (the 'woolly rhino') and *Ceratotherium neumayri*. Similar annular rugosities have been described and figured for *Punjabitherium* (Khan 1971) and the stem taxon *Gaindatherium* (Colbert 1934), placing the first occurrence of horns at 16–20 Ma, approximately 20 Ma after the first evidence of dermal body armor (Fig. 2-5). This timing rules out the possibility that rhinoceros dermal armor is an adaptive response to horn use in agonistic behavior (Larson and Losos 1996).

Evolutionary history of rhinocerotid dermal armor

The use of sharpened tusks in intraspecific agonistic behaviors has been cited as a possible selection pressure driving the evolution of dermal body armor (Shadwick et al. 1992), and shearing tusks occur convergently in many of the extant mammalian taxa that possess this derived dermal morphology (Schumacher 1931; Sokolov 1982). We present

the results of two phylogenetic comparative tests that address the premise and support for adaptive explanations, respectively: (a) a lineage test that maps the relative positions of the putative selection regime and adaptation on a phylogeny (selection regime must closely precede adaptation to be a valid adaptive explanation (Larson and Losos 1996); and (b) a convergence test that examines whether independent occurrences of the selection regime are accompanied by the putative adaptation more often than would be expected by chance (Pagel 1994).

A lineage test for adaptive relationship between shearing tusks and the bony indicator for dermal armor in rhinocerotids (Cerdeño 1995; Antoine 2002; Antoine et al. 2003; Maddison and Maddison 2006a, b) shows that the two traits are closely related, with dermal armor appearing in *Trigonias* spp. approximately 4 Ma after the first evidence of shearing tusks in their immediate basal outgroup *Teletaceras* (Fig. 2-5), indicating that an adaptive relationship is plausible. A convergence test of this same relationship among extant mammals (Sokolov 1982; Nowak and Paradiso 1983; Pagel 1994; Arnason and Janke 2002; Fernández and Vrba 2005; Kriegs et al. 2006) shows significant character correlation ($p = 0.005$; Fig. 2-8), indicating a degree of convergence best explained by adaptation. Tusks and dermal armor both initially develop as sexually dimorphic characters in basal rhinocerotids, and tusks, not horns, remain the primary offensive weapons of the three basal extant rhinoceros species (Dinerstein 1991; Prothero and Schoch 2002), further supporting the relationship of shearing tusks as the selection pressure and dermal armor as the adaptive response. The evolution of these two traits in rhinocerotids is thus convergent with the evolution of analogous sexually dimorphic traits

in other mammals with highly territorial males such as swine, hippopotamus, and elephant seals.

Evolutionary history of rhinoceros horns

This finding falsifies a part of the previously held adaptive hypothesis for rhinoceros horn evolution in that the intrasexual selection pressures previously used to explain this event (Janis 1982) are in place by the late Eocene, that is, well in advance of the appearance of horns. Nevertheless, an early Miocene date for horn evolution in rhinoceros is highly congruent with the timing of horn and antler evolution in other ungulates. The first appearance of rhinocerotid horns (as marked by *Gaindatherium* at 16–20 Ma) coincides closely with the independent appearance of horn-like cranial appendages in six other ungulate lineages, and all of these events occur within 5 Ma of the onset of regional increases in the prominence of grassland habitat (Fig. 2-5; Janis and Scott 1987; Jacobs et al. 1999). Although it is currently unclear what mechanism drives the evolution of horns in ungulates, and indeed whether or not the same mechanism is acting on all seven convergent lineages, the similarity in timing and degree of convergence between these lineages suggests a common cause, perhaps relating to enhanced visual communication in their newly more open habitats. The temporal relationship between the appearance of horns and the spread of more open savannah habitats is further corroborated by the timing of increased cheek tooth crown height (mesodonty–hypsodonty) in many ungulate lineages, including several rhinocerotid taxa. Hypsodonty is strongly correlated with grass-rich diet in extant mammals (Janis 1988)—the independent increases in crown height in rhinocerotid lineages tracks their transition

from closed and mixed habitats to more open, grass-rich habitats during the early and middle Miocene (Fig. 2-9).

Conclusions

The architecture of the dermis that first evolved as an adaptation to produce body armor was later co-opted (exaptation) in the region covering the nasal and frontal bones in rhinocerotids to produce a support for massive keratinous horns (Fig. 2-5). Although the internal structure and dermal support of rhinocerotid horns are novel features, their external form and the ecological context of their first appearance are convergent with primitive horns and antlers in other ungulate lineages. The novel features of rhinoceros horns are thus not the result of a single novel selection pressure, but instead arise from a sequential combination of two commonly occurring selection pressures. Both the adaptive and the exaptive events in this scenario are convergent on adaptive responses in other large mammal groups. Thus, a more detailed view of rhinoceros skin evolution adds another layer to the iconic one- or two-horn adaptation model (Lewontin 1978; Coddington 1990), emphasizing the importance of combinatorial processes in the origin of novelty.

Materials and Methods

Anatomy and histology of horn attachment

No detailed descriptions of rhinoceros horn attachment are available in the anatomical literature. Bony characters pertaining to skin and horns were examined in skeletal specimens representing all five extant rhinoceros taxa, all four extant tapir taxa, and four extant equid taxa (together composing an ingroup sample of 116 individuals;

Appendix A), as well as a number of extant mammalian taxa with similar bony characters and their sister taxa (outgroup sample, 71 individuals in 11 taxa; Appendix A), to separate skin-related bone morphology from individual and/or phylogenetically controlled variation. We then examined the nasal and frontal horn bosses and adjacent skin and bone of one specimen of *Ceratotherium simum* (OUVC 9541) by dissection, histology, and x-ray computed tomography (CT scanning) to document the pattern of soft-tissue elaboration and ossification that produces the characteristic rugose bone surfaces of rhinoceros skulls.

Analysis of fossil material

Twenty-five extinct ceratomorph taxa (63 individuals; Appendix A) were examined for skin-related characters identified from extant specimens. Presence/absence and homogeneity/annularity of rugose bone patches were scored as binary categorical characters in Mesquite v1.12 (Maddison and Maddison 2006a) with asymmetrical two-parameter models of character state change. We generated a matrix representation with parsimony (MRP; Ragan 1992) supertree of rhinocerotids (Swofford 2001; Maddison and Maddison 2006a) from existing morphological and molecular phylogenies (Morales and Melnick 1994; Cerdeño 1995; Tougard et al. 2001; Antoine 2002; Antoine et al. 2003; Orlando et al. 2003), and trimmed this tree to encompass the 24 extant and extinct rhinocerotid taxa of our sample. Taxon appearance times were fixed using locality data from specimens in our sample as well as occurrence data downloaded from the Paleobiology Database. Confidence intervals around taxon first appearances were calculated using the method of Strauss and Sadler (1989). Internal branches nearest to

terminal taxa were set at 1 Ma, placing internal nodes close to documented fossil occurrences. We then reconstructed ancestral character states with a maximum likelihood criterion onto this phylogeny (Maddion and Maddison 2006b), both with branch lengths in Ma and with all branch lengths set to one (no substantive difference exists between these reconstructions). First appearances of traits reported here correspond to the more conservative indicator of a confidence interval around the first fossil evidence for a trait, not the reconstruction of the trait at a node.

Lineage test for adaptation

For the lineage test, we imported mesial dentition characters (an organismal proxy for the putative selection regime) from published sources (Cerdeño 1995; Antoine 2002; Antoine et al. 2003) into Mesquite v1.12 as binary categorical characters with asymmetrical two-parameter models of character state change and reconstructed ancestral character states with a maximum likelihood criterion. We then compared the order of appearance and temporal separation of shearing tusks (selection regime) and dermal armor (adaptation). The appearance of dermal armor more basal than shearing tusks would falsify a hypothesis of dermal armor as an adaptive response (Larson and Losos 1996). No strict criteria for interpreting temporal separation between selection regime and adaptive response exist, beyond the conceptual model that adaptation should accompany selection regime in 'short order.' Spans of 5 Ma between selection regime and adaptation in the Miocene record have been discussed as problematic (Strömberg 2006), although interpretations depend upon the temporal resolution of fossil occurrences and the degree of uncertainty that surrounds the first appearance of a trait in a fossil taxon.

Convergence test for adaptation

For the convergence test, we imported data on mesial dentition (Nowak and Paradiso 1983) and dermal morphology (Sokolov 1982) in representative mammalian species from published sources into Mesquite v1.12, and placed these taxa in a composite higher-level phylogeny of mammals (Arnason and Janke 2002; Fernández and Vrba 205; Kriegs et al. 2006) with all branch lengths set to one to reflect uncertainty in rates of morphological change. Correlation between shearing tusks and dermal armor was tested in this phylogenetic framework using Pagel's Omnibus test with 10 likelihood searches and 1000 Markov chain Monte Carlo replicates (Pagel 1994; Maddison and Maddison 2006a).

Assessing temporal congruence

We examined congruence in the timing of horn evolution between artiodactyl and rhinocerotid lineages by comparing the interval for the first appearance of horns in *Gaindatherium* with Strauss and Sadler (1989) confidence intervals for the earliest representative taxon for each occurrence of horns or antlers in artiodactyls (Janis 1982; Janis and Scott 1987) . We then compared the dates of these intervals with published dates for the spread of grassland habitat by continent (Jacobs et al. 1999). Ancestral states for a composite cheek tooth height character (Cerdeño 1995; Antoine 2002; Antoine et al. 2003) were calculated on the complete rhinocerotid supertree using a symmetrical one-parameter character model and a likelihood criterion, and likelihood ratios for low vs. high cheek teeth were mapped onto nodes of the trimmed supertree to determine independent occurrences of mesodonty or hypsodonty.

Literature Cited

Antoine P-O 2002. *Phylogénie et évolution des Elasmotheriina (Mammalia, Rhinocerotidae.)* Paris: Publications scientifiques du Muséum.

Antoine P-O, Duranthon F, Wellcome J-L. 2003. *Alicornops* (Mammalia, Rhinocerotidae) dans le Miocene superieur des Collines Bugti (Balouchistan, Pakistan): implications phylogenetiques. GEODIVERSITAS 25:575–603.

Arnason U, Janke A. 2002. Mitogenomic analyses of eutherian relationships. Cytogenetic and Genome Research 96:20.

Berger J, Cunningham C. 1998. Natural variation in horn size and social dominance and their importance to the conservation of black rhinoceros. Conservation Biology 12:708–711.

Cerdeño E. 1995. Cladistic analysis of the family Rhinocerotidae (Perissodactyla). American Museum Novitates 3143:1–25.

Coddington JA. 1990. Bridges between evolutionary pattern and process. Cladistics 6:379–386.

Colbert EH. 1934. A new rhinoceros from the Siwalik beds of India. American Museum Novitates 749:1–13.

Deng T. 2005. New discovery of *Iranotherium morgani* (Perissodactyla, Rhinocerotidae) from the late Miocene of the Linxia Basin in Gansu, China, and its sexual dimorphism. Journal of Vertebrate Paleontology 25:442–450.

Dinerstein E. 1991. Sexual dimorphism in the greater one-horned rhinoceros (*Rhinoceros unicornis*). Journal of Mammalogy 72:450–457.

Fernández MH, Vrba ES. 2005. A complete estimate of the phylogenetic relationships in Ruminantia: a dated species-level supertree of the extant ruminants. Biological Reviews 80:269–302.

Hieronymus TL, Witmer LM, Ridgely RC. 2006. Structure of white rhinoceros (*Ceratotherium simum*) horn investigated by X-ray computed tomography and histology with implications for growth and external form. Journal of Morphology 267:1172–1176.

Jacobs BF, Kingston JD, Jacobs LL. 1999. The origin of grass-dominated ecosystems. Annals of the Missouri Botanical Garden 86:590–643.

Janis CM. 1982. Evolution of horns in ungulates: ecoogy and paleoecology. Biological Reviews 57:261–318.

Janis CM. 1988. An estimation of tooth volume hypsodonty indices in ungulate mammals, and the correlation of these factors with dietary preference. In: Russell DE, Santoro J-P, Sigogneau-Russell D, editors. Teeth Revisited, Proceedings of the VIIth International Symposium on Dental Morphology. Paris: Mémoires du Muséum d'Histoire Naturelle Séries C. p. 367–387.

Janis CM, Scott KM. 1987. The interrelationships of higher ruminant families, with special emphasis on the members of the Cervoidea. American Museum Novitates 2893:1–85.

Khan E. 1971. *Punjabitherium* gen. nov.: An extinct rhinocerotid of the Siwaliks (Punjab, India). Proceedings of the Indian Natural Sciences Academy 37A:105–109.

Kingdon J. 1979. East African mammals: An atlas of evolution in Africa. Vol.3. Part B, Large mammals London: Academic Press.

Kriegs JO, Churakov G, Kiefmann M, Jordan U, Brosius J, Schmitz J. 2006. Retroposed elements as archives for the evolutionary history of placental mammals. PLoS Biology 4:e91.

Larson A, Losos JB. 1996.Phylogenetic systematic of adaptation. In: Rose MR, Lauder GV, editors. Adaptation. San Diego: Academic Press. p. 187–220.

Lewontin RC. 1978. Adaptation. Scientific American 239:212–222.

Maddison WP, Maddison DR. 2006a. Mesquite: a modular system for evolutionary analysis, v1.12 (http://mesquiteproject.org).

Maddison WP, Maddison DR. 2006b. StochChar: a package of Mesquite modules for stochastic models of character evolution, v1.1 (http://mesquiteproject.org).

Morales JC, Melnick DJ. 1994. Molecular systematics of the living rhinoceros. Molecular Phylogenetics and Evolution 3:128–134.

Nowak RM, Paradiso JL. 1983. Walker's mammals of the world. Baltimore: Johns Hopkins University Press.

Orlando L, Leonard JA, Thenot A, Laudet V, Guerin C, Hänni C. 2003. Ancient DNA analysis reveals woolly rhino evolutionary relationships. Molecular Phylogenetics and Evolution 28:485–499.

Pagel M. 1994. Detecting correlated evolution on phylogenies: A general method for the comparative analysis of discrete characters. Proceedings of The Royal Society B Biological Sciences 255:37.

Prothero DR, Schoch RM. 2002. Horns, tusks, and flippers: The evolution of hoofed mammals. Baltimore: Johns Hopkins University Press.

Rachlow JL, Berkeley EV, Berger J. 1998. Correlates of male mating strategies in white rhinos (*Ceratotherium simum*). Journal of Mammalogy 79:1317–1324.

Ragan MA. 1992. Phylogenetic inference based on matrix representation of trees. Molecular Phylogenetics and Evolution 1:53–58.

Ryder ML. 1962. Structure of rhinoceros horn. Nature 193:1199–1201.

Schumacher Sv. 1931. Integument der Mammalier. In: Bolk L, Goppert E, Kallius E, Lubosch W, editors. Handbuch der Vergleichenden Anatomie der Wirbeltiere. Berlin: Urban und Schwarzenburg. p. 449–504.

Shadwick RE, Russell AP, Lauff RF. 1992. The structure and mechanical design of rhinoceros dermal armour. Philosophical Transactions of the Royal Society of London. Series B, Biological sciences 337:419–428.

Sokolov VE. 1982. Mammal skin. Berkeley: University of California Press.

Strauss D, Sadler PM. 1989. Classical confidence intervals and Bayesian probability estimates for ends of local taxon ranges. Mathematical Geology 21:411–427.

Strömberg CAE. 2006. Evolution of hypsodonty in equids: testing a hypothesis of adaptation. Paleobiology 32:236–258.

Swofford DL. 2001. PAUP*: phylogenetic analysis using parsimony (*and other methods), v4.10b. Sunderland: Sinauer Associates.

Tougard C, Delefosse T, Hänni C, Montelgard C. 2001. Phylogenetic relationships of the five extant rhinoceros species (Rhinocerotidae, Perissodactyla) based on

mitochondrial cytochrome b and 12S rRNA genes. Molecular Phylogenetics & Evolution 19:34–44.

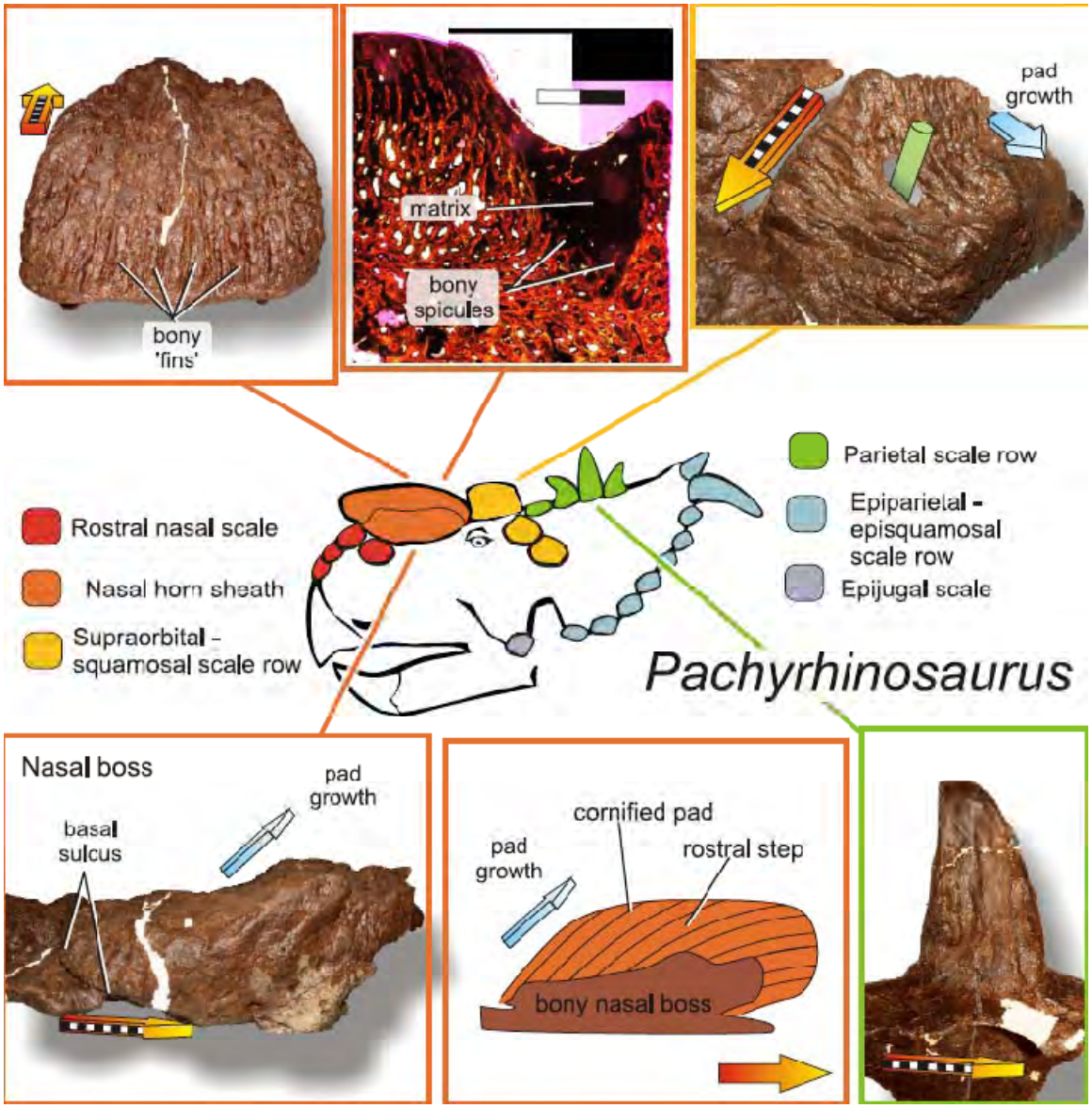

Figure 5-12. (A) Skin structures inferred for *Pachyrhinosaurus*. Scale bars are 10 cm with arrowhead pointing rostrally, unless otherwise noted. (B) Caudal view of the nasal boss of TMP 86.55.206 *P. lakustai*, showing bony "fins" indicative of a cornified pad growing at a low angle to the bone surface. (C) Histological section of a bony "fin" and sulcus from the nasal boss of *P. lakustai*, showing infill of matrix and fine bone spicules; compare to Figure 5-8C. Scale bar is 2mm. (D) Supraorbital boss of TMP 89.55.427 *P. lakustai*, showing bony "fins" and communication with frontal sinus (green bar). Blue arrow shows inferred growth direction for the overlying cornified pad. (E) Nasal boss of TMP 89.55.427 *P. lakustai*, showing basal sulcus and bony "fins" at the caudal end of the boss. The nasal boss of this specimen is very similar to an adult *Achelousaurus* nasal boss (Fig. 5-11D). (F) Schematic of inferred cornified tissue on the bony nasal boss of *Pachyrhinosaurus* spp. (G) Parietal horn of TMP 86.55.258 *P. lakustai*.

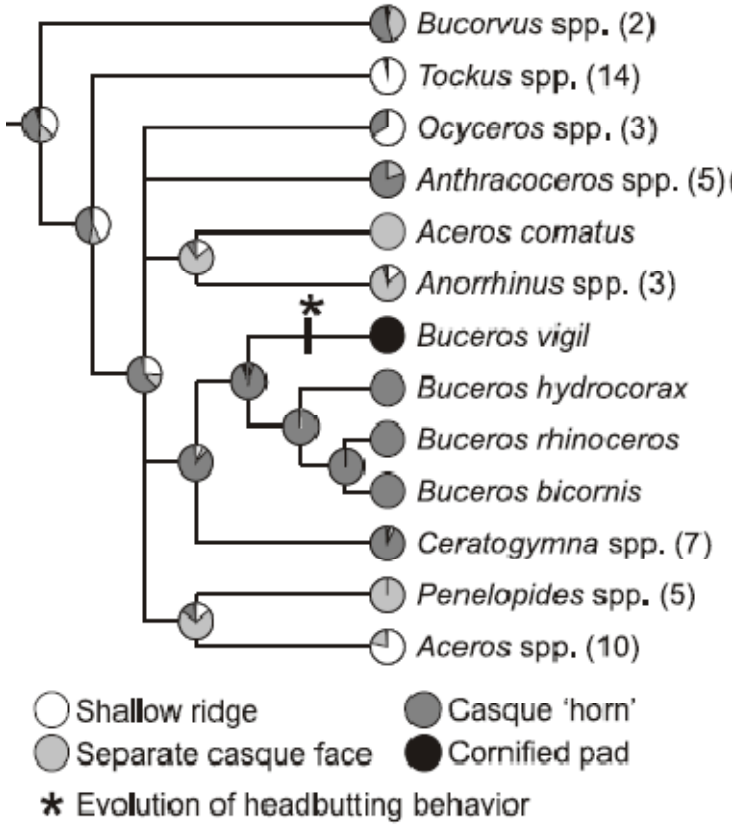

Figure 5-13. Ancestral character state reconstructions of casque morphology and headbutting behavior in Bucerotidae (hornbills). A casque with a projecting "horn" is unequivocally reconstructed for *Ceratogymna+Buceros*, and the transition to a cornified pad in *Buceros vigil* is accompanied by a transition from light bill clashing to headbutting behaviors (asterisk). Nodes show proportional likelihoods for each morphological character state with Pagel (1992) transformed branch lengths. Topology after Kemp (1995).

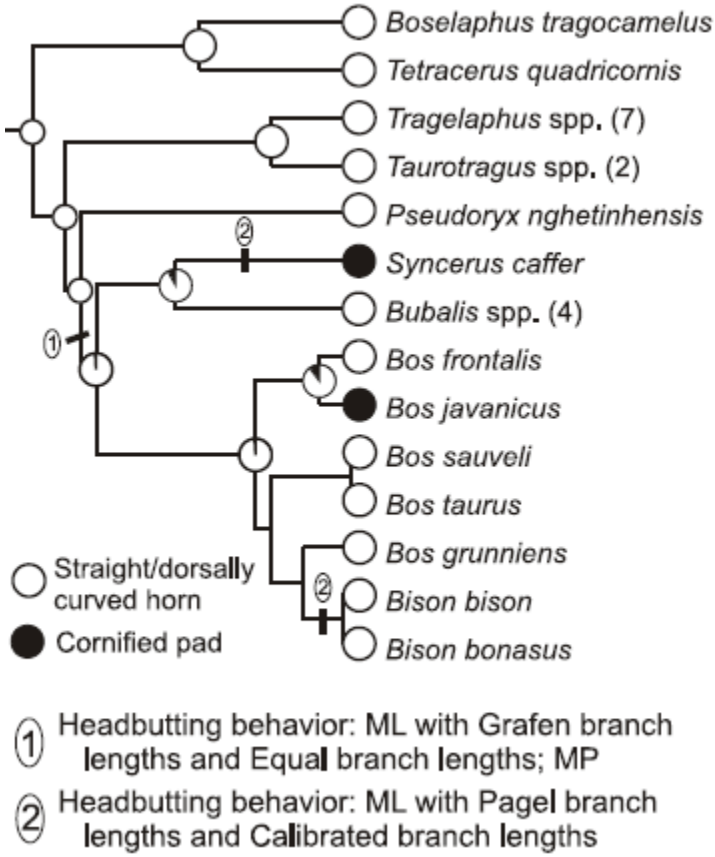

Figure 5-14. Ancestral character state reconstructions of horn morphology and headbutting behavior in Bovinae (cattle and allies). The transition to a cornified pad in *Syncerus* is associated with an increase in the intensity of headbutting and charging behavior compared to related taxa, but the domestication of some forms of *Bubalis* and *Bos* and a paucity of behavioral data for the remaining members of Bovini contribute to a low-resolution picture of the relationship between horn morphology and agonistic behavior in this clade. Nodes show proportional likelihoods for each morphological character state with the published topology and branch lengths of Fernández and Vrba (2005). The topology of Hassanin and Ropiquet (2004) was also used for this test.

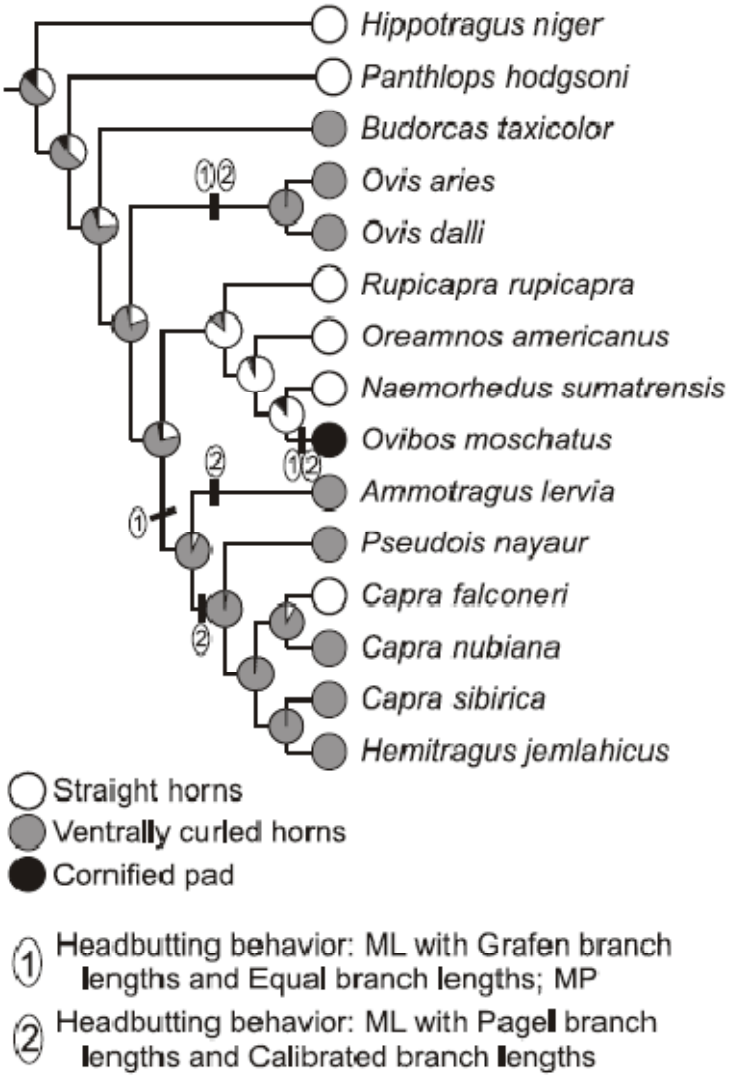

Figure 5-15. Ancestral character state reconstructions of horn morphology and headbutting behavior in Caprinae (goats and sheep) and outgroups. Most unequivocal reconstructions of ventrally curved horns (*Ovis*, *Ammotragus*, and *Capra+Pseudois* in this example) are matched by unequivocal reconstructions of headbutting behavior, as is the transition from straight horns to cornified pads in *Ovibos*. Node show proportional likelihoods for each morphological character state with Pagel (1992) transformed branch lengths and the topology of Ropiquet and Hassanin (2005). The topology of Lalueza-Fox et al. (2005) was also used for this test.

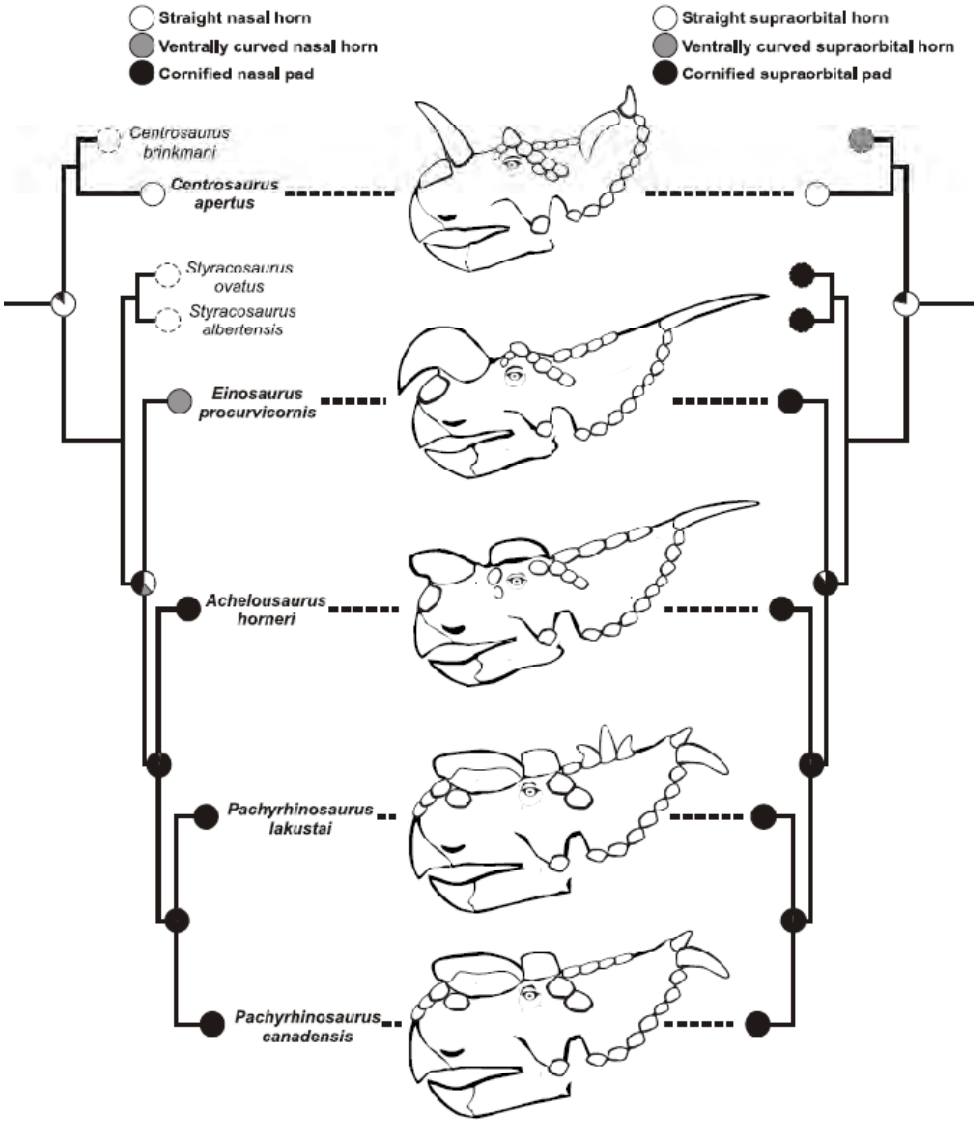

Figure 5-16. ML Ancestral character state reconstructions of nasal (A) and supraorbital (B) horn morphology in centrosaurine dinosaurs. The transition from straight horns in basal centrosaurines to ventrally curved nasal horns and cornified pads in derived centrosaurines is very similar to the morphological transitions associated with headbutting behavior in extant caprines. The primitive polymorphism of supraorbital horn cores in *Centrosaurus* (Sampson et al. 1997) is canalized in more derived centrosaurines, and this development is followed by the progression of ventrally curved nasal horns and cornified pads in *Einiosaurus*, *Achelousaurus*, and *Pachyrhinosaurus*. Character states for *Centrosaurus brinkmani*, *Styracosaurus ovatus*, and *Styracosaurus albertensis* were taken from published descriptions, and were not included in ancestral character state reconstructions.

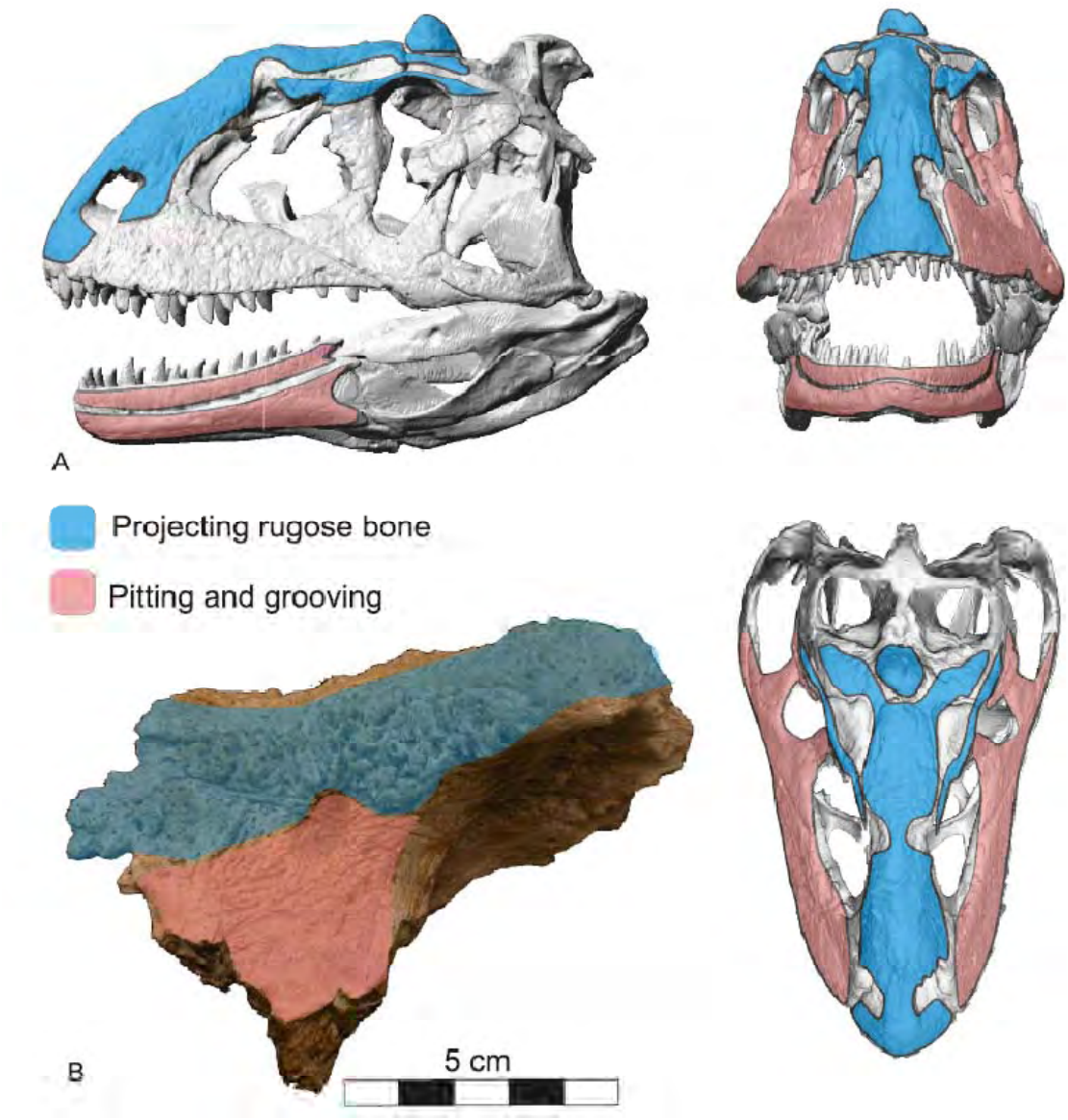

Figure 6-1. Surface rendering of the skull of *Majungasaurus crenatissimus* (FMNH PR 2100), showing (A) areas of pitting and grooving on the lateral surface of the face (red) as distinguished from projecting rugose bone across the skull roof (blue). Inset in (B) shows projecting rugose bone texture on the dorsal part of the lacrimal in UA 8718.

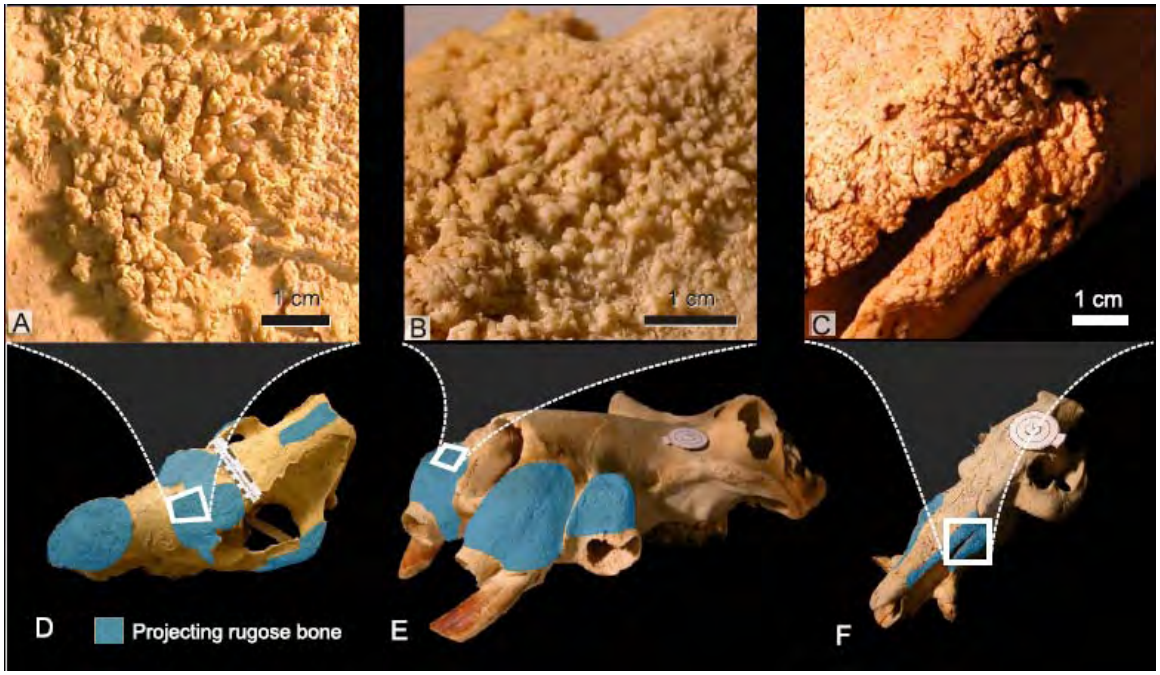

Figure 6-2. Skulls of *Dicerorhinus* (Sumatran rhino; A, D), *Hippopotamus* (B, E), and *Potamochoerus* (red river hog; C, F), all in oblique left rostrolateral view, showing projecting rugose bone (A–C) and its distribution (D–F). Scale bar on D is 14 cm; round scale bars on E and F are 6 cm in diameter.

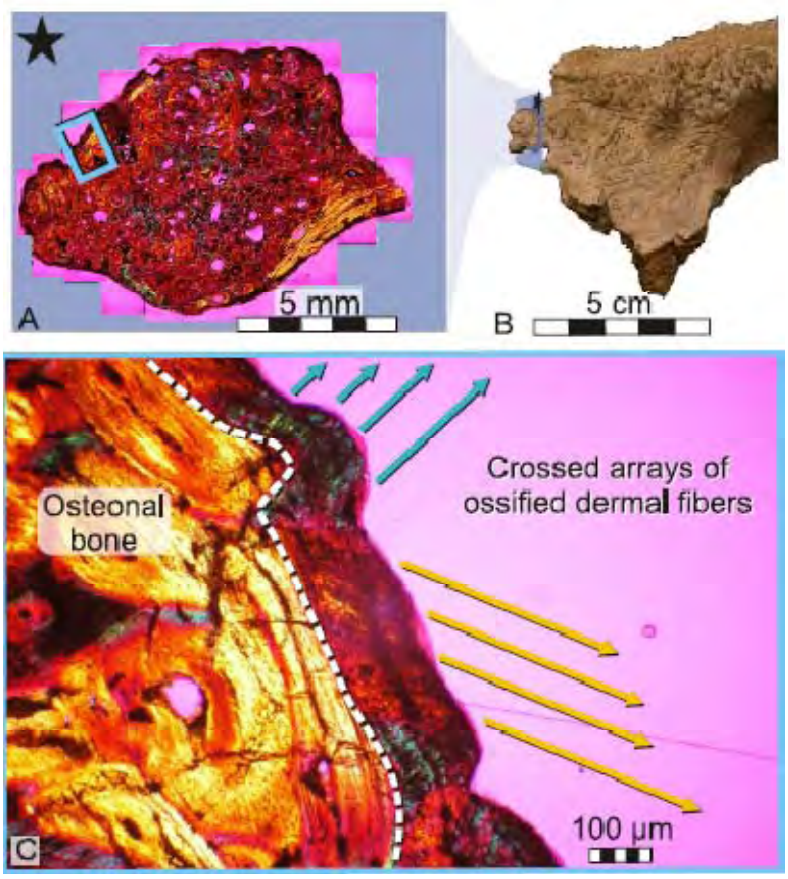

Figure 6-3. Paleohistology of projecting rugose bone in *Majungasaurus crenatissimus* (UA 8718). A lateral view of the left lacrimal (B) shows the plane of section (A), with the star in the upper left marking the dorsolateral corner of the section. Inset at bottom (C) shows an external "rind" of dermal ossification (dashed line) composed of crossed arrays of ossified dermal collagen fiber bundles ranging from 50–200 µm in diameter. Yellow and blue arrows show bundle orientations.

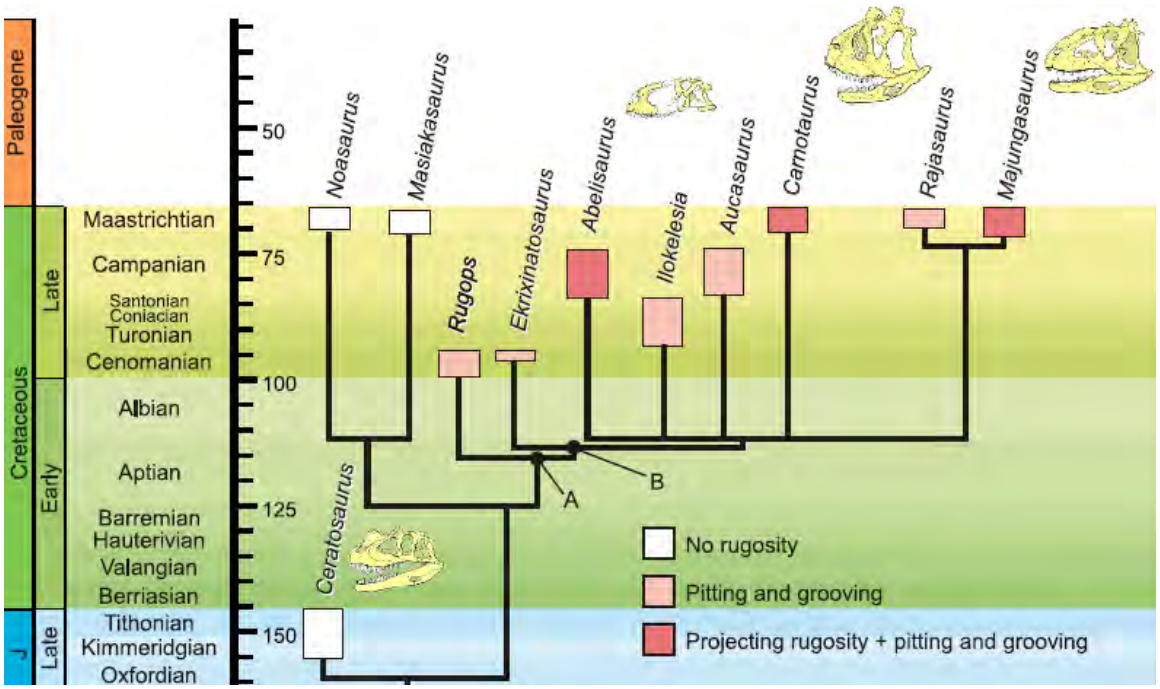

Figure 6-4. Phylogenetic and stratigraphic context for the evolution of CADA in *Majungasaurus* and other abelisaurids. Placement of the ancestral state for several cephalic characters that may also reflect more violent agonistic behaviors are shown as reconstructed by parsimony: (A) retreat of the antorbital fossa from the dorsolateral margin of the maxilla; presence of dermal bone covering the lacrimal fossa; grooving on interdental plates. (B) Presence of suborbital flange of the postorbital bone; presence of dermal bone covering the squamosal-postorbital contact. Topology, divergence dates, and character states in A and B after Carrano and Sampson (2008).

APPENDIX A: SUPPLEMENTARY INFORMATION FOR CHAPTER 2

Data for comparative analyses were downloaded from the Paleobiology Database (www.paleodb.org) on 24 February, using the following parameters: output data = occurrence matrix; taxa to include = trigonias, gaindatherium, aletomeryx, climacoceras, syndyoceras, dicrocerus, eotragus, paleomeryx, paracosoryx; timescale = Gradstein 7: stages; include preservation categories = regular taxon, form taxon.

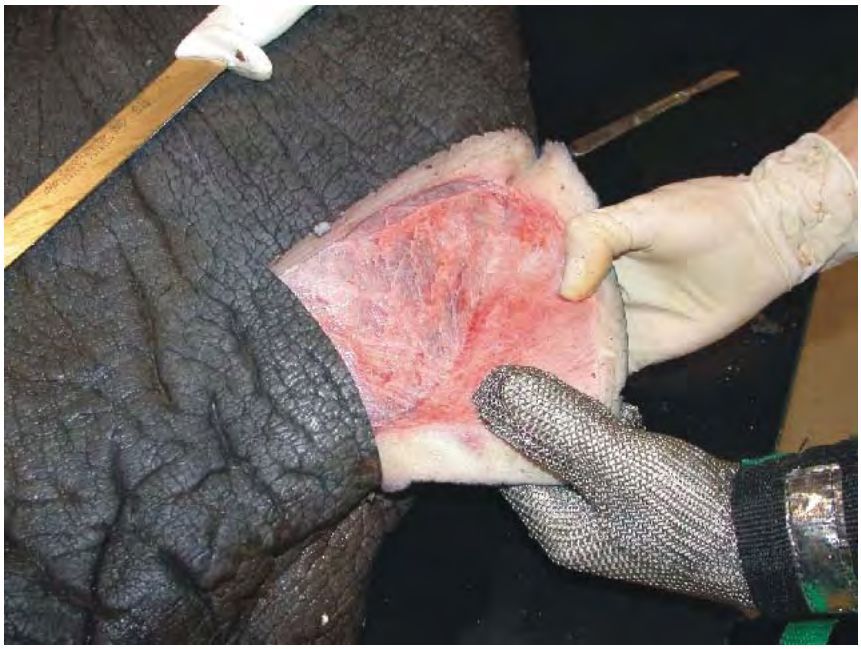

Figure A-1. A portion of skin overlying the left cheek region of a white rhinoceros (*Ceratotherium simum*, Ohio University Vertebrate Collections [OUVC] 9541). This sample is representative of skin thickness across the rest of the head and much of the body for extant rhinoceros taxa. In addition to the marked difference in thickness when compared to the dermis of other mammals, rhinoceros dermis is composed of crossed arrays of large-diameter collagen fibers, imparting increased stiffness and strength to the tissue (Shadwick et al. 1992).

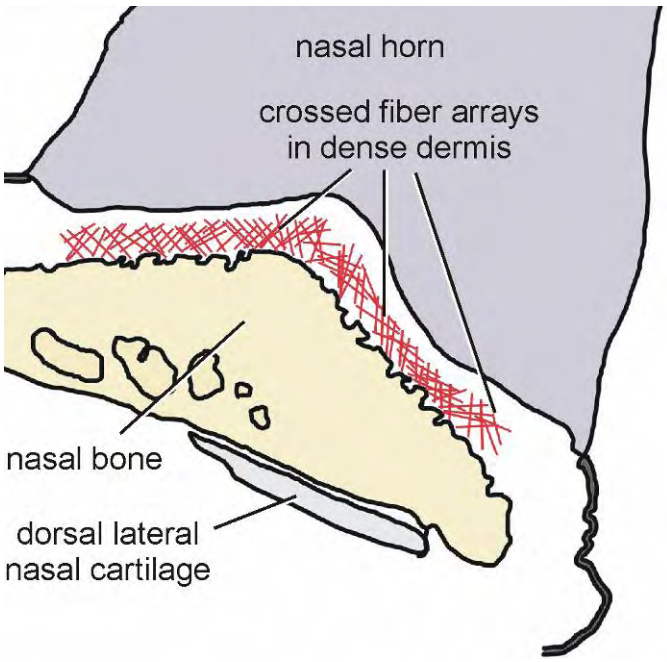

Figure A-2. Schematic representation of dermal fiber bundle orientations at the midline beneath the nasal horn of white rhinoceros (*Ceratotherium simum*, OUVC 9541), showing crossed fiber arrays. Fiber bundles along the midline are predominantly oriented along the sagittal plane.

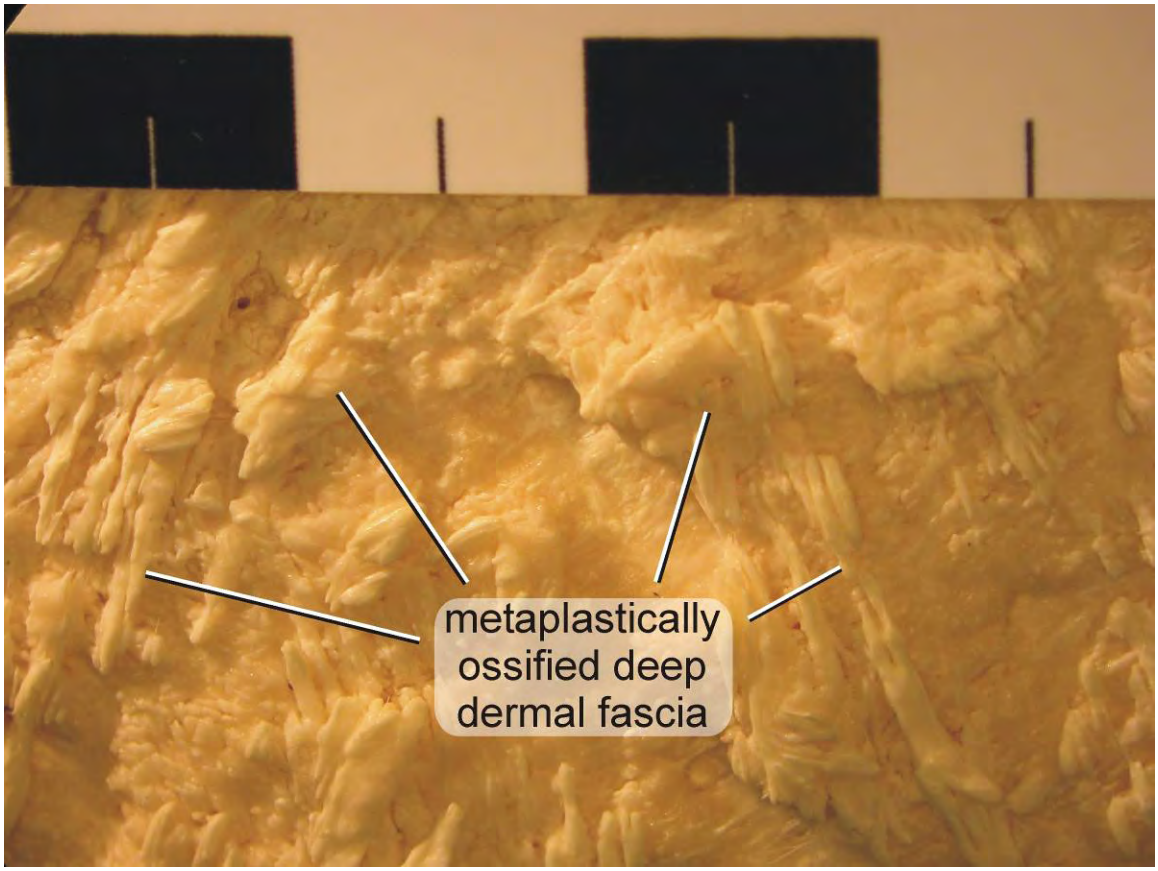

Figure A-3. Cleaned bone surface from beneath frontal horn of white rhinoceros (*Ceratotherium simum*, OUVC 9541). Much of the rugose texture visible on the bone surface is the result of metaplastic ossification, or bone growth within existing connective tissue (Haines and Mohuiddin 1968) of the deep dermal fascia (= superficial fascia of human anatomy). Scale bar increments equal 1 cm.

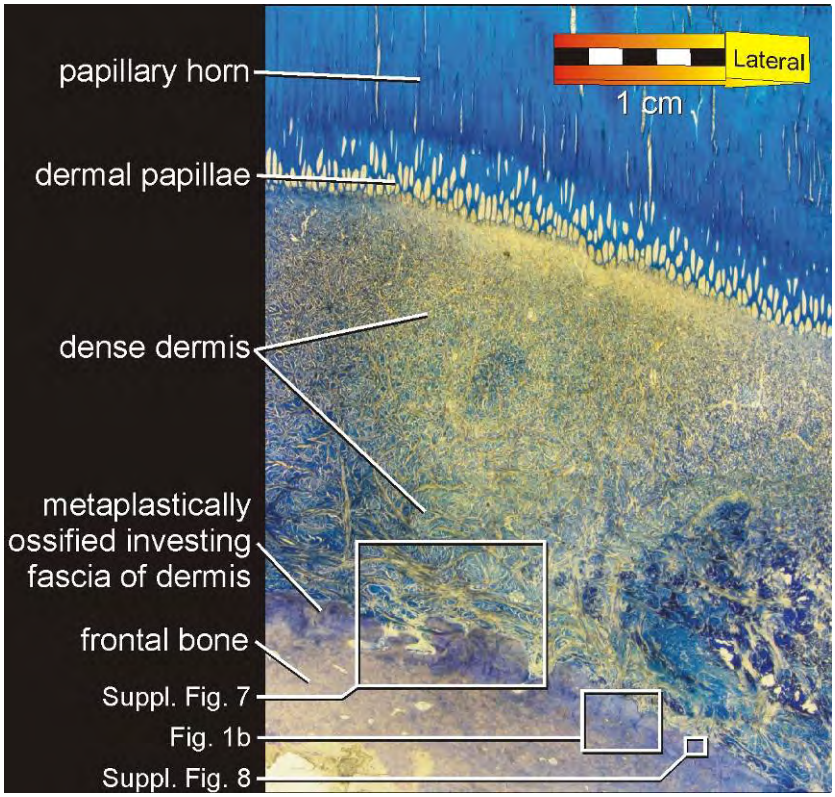

Figure A-4. Plan view of transverse cross-sectional histology beneath the frontal horn of a white rhinoceros (*Ceratotherium simum*, OUVC 9541). Histological sections for this study were cut from polymethylmethacrylate (PMMA) plastic embedded tissue blocks, polished, and surface stained with Toluidine Blue O. Illumination for this image was provided by unaltered white light. The individual tubules of cornified epidermis that make up the horn (Ryder 1962) are clearly visible, especially at the base of the horn where they surround dermal papillae. The reticular or dense dermis beneath the horn shows a gradient in collagen fiber bundle size between approximately 50 μm near the horn and approximately 700 μm near the underlying bony attachment. Inset boxes show the areas displayed in other figures.

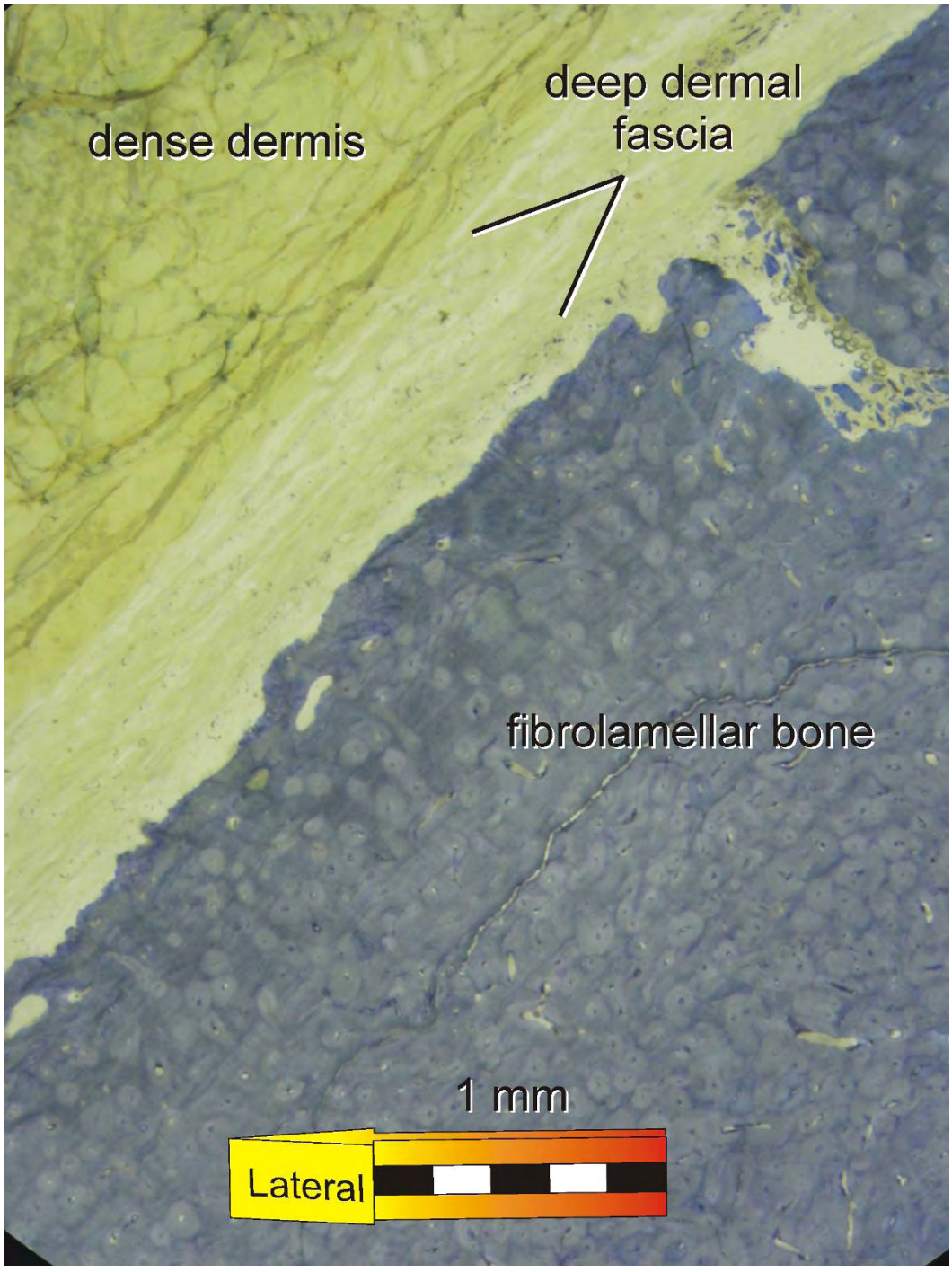

Figure A-5. Bone-dermis border from behind the frontal horn, illuminated with unaltered white light. This section was taken approximately 4 cm caudal to the edge of the frontal horn, and shows fibrolamellar bone extending to the periosteal surface, with the absence of metaplastically ossified dermis. A thick deep dermal fascia merges with the periosteum here. In other locations of the skull, as over the origin of *M. levator nasolabialis*, the deep dermal fascia leaves the bone surface and continues over the epimysium.

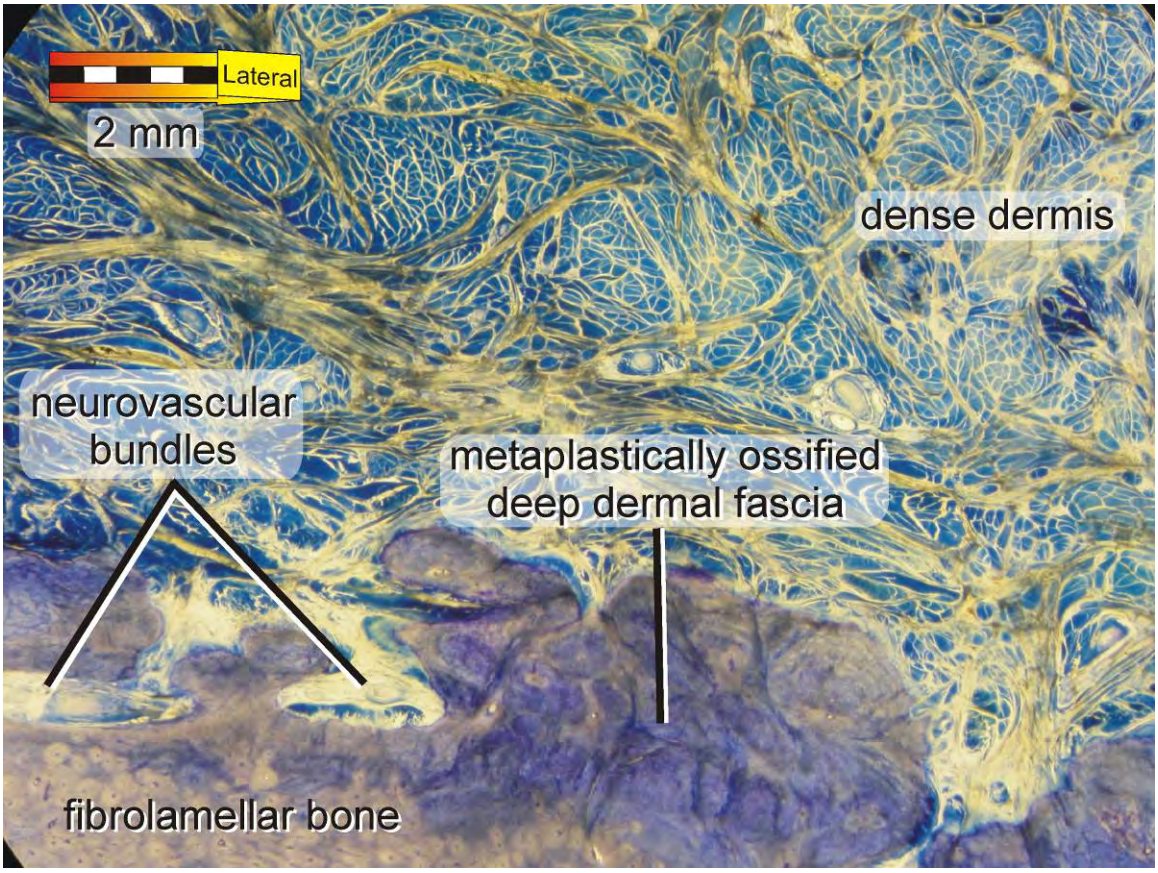

Figure A-6. Detail of the transverse section in Fig. 54, illuminated by unaltered white light. The rugose border between ossified tissues (purple) and soft tissues (blue) can be seen clearly in this image. Appositional growth around neurovascular bundles creates some of the rugosity associated with rhinoceros horn attachment. Other rugose areas (dark purple) are the result of uneven metaplastic ossification of the deep dermal fascia.

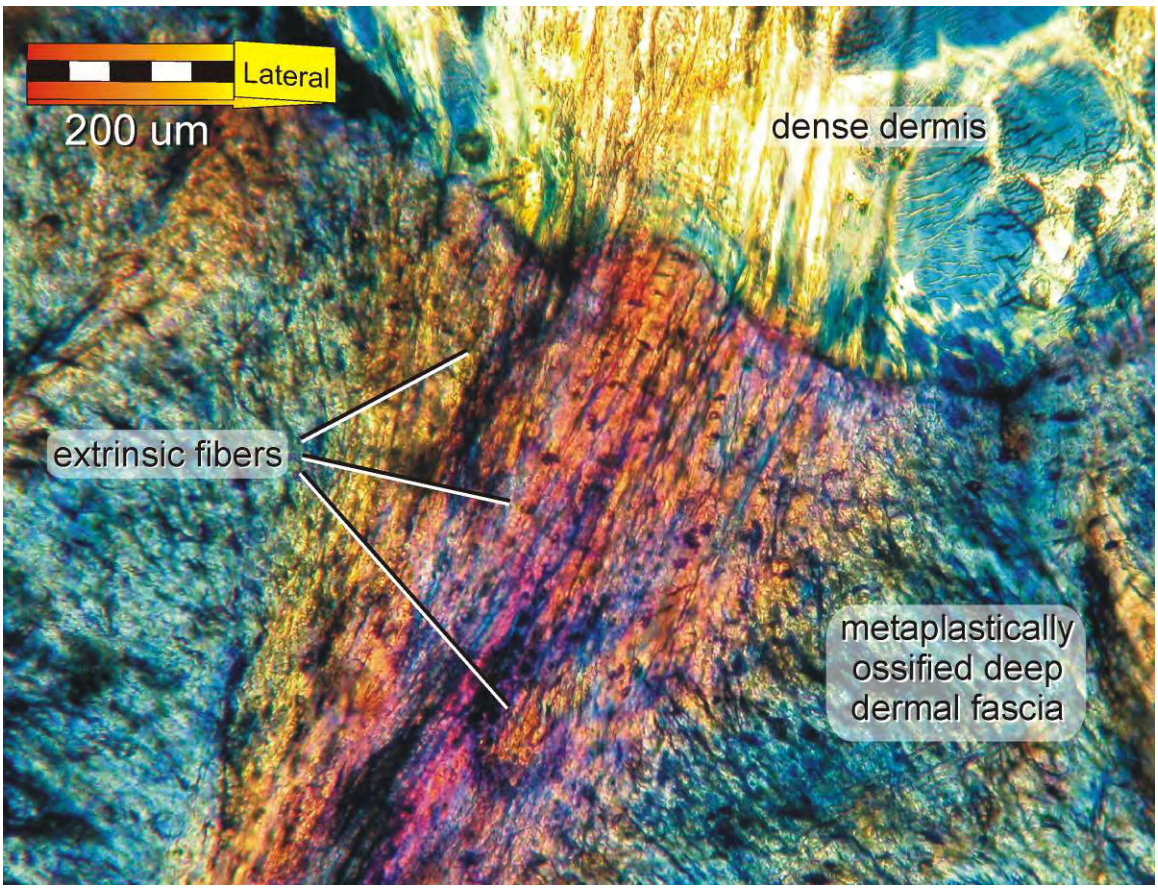

Figure A-7. Detail of the transverse section in Fig. 54, viewed under crossed polarizers with a ¼ wave plate. In this image, different fiber orientations have resulted in different interference colors, allowing normally-oriented extrinsic fibers from the dense dermis (purple-red) to be differentiated from the tangentially-oriented fibers of the metaplastically ossified deep dermal fascia. This arrangement of tissue is similar to the fibrous entheses found at some muscle and ligament attachments (Benjamin et al. 2002).

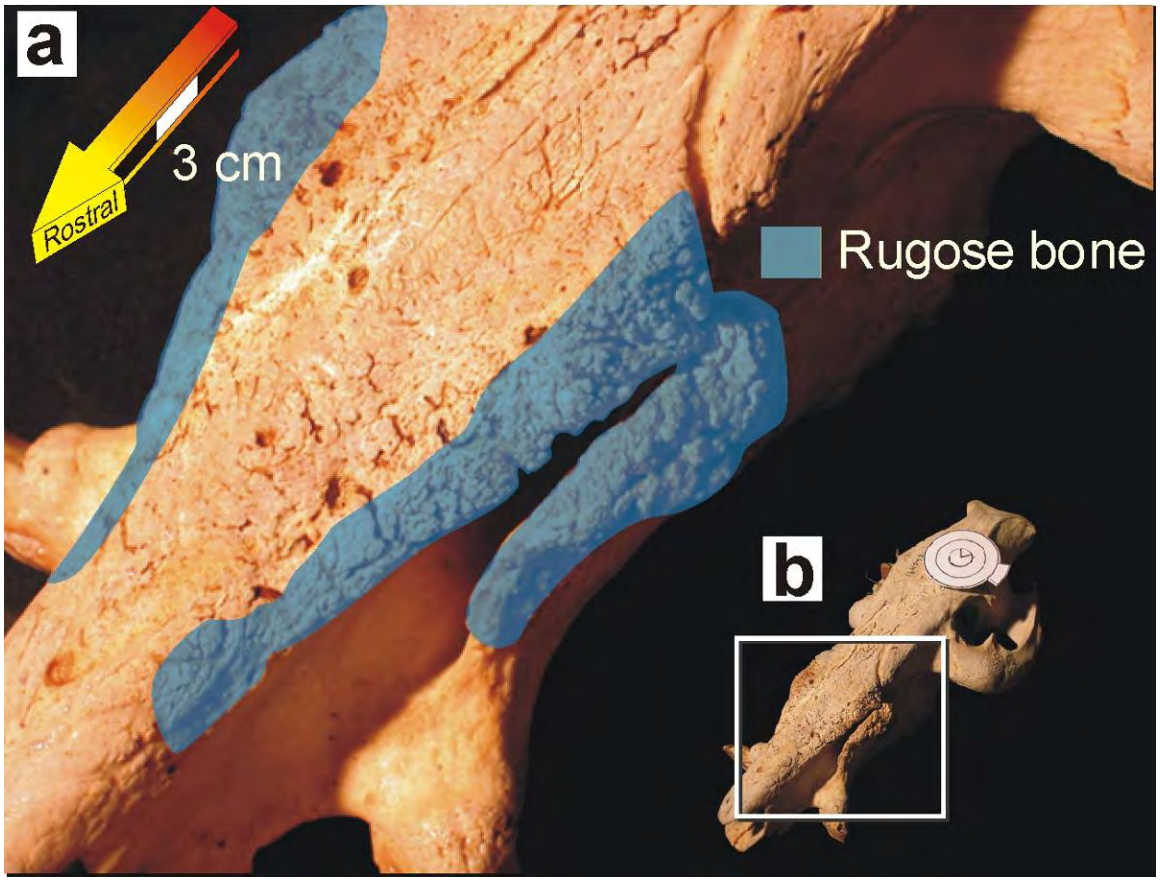

Figure A-8. Rugose bone on the maxillae and nasals of the red river hog *Potamochoerus porcus*, USNM 164542. **a.** As in *Hippopotamus*, *Potamochoerus* displays patches of rugose bone around the canine fossa of the maxilla. The extent of rugose bone closely matches the area of skin that is most often in contact with aggressors during agonistic behaviors (Kingdon 1979). In addition to the gross similarity of these rugose patches to those seen on extant and extinct rhinocerotids, the histological structure of the overlying dermis in hippopotamids and suiforms is also similar to that in extant rhinocerotids, showing prominent crossed fiber arrays (Schumacher 1931;Sokolov 1982; Shadwick et al. 1992). Although the dermal and bony morphologies of these animals are very similar, they have very different degrees of epidermal elaboration (massive horns vs. thin pliable epidermis), suggesting that dermal metaplasia is not a sufficient bony indicator for horns, but instead provides a clear bony indicator for dermal body armor. **b.** Inset box shows the location of **a** on the skull.

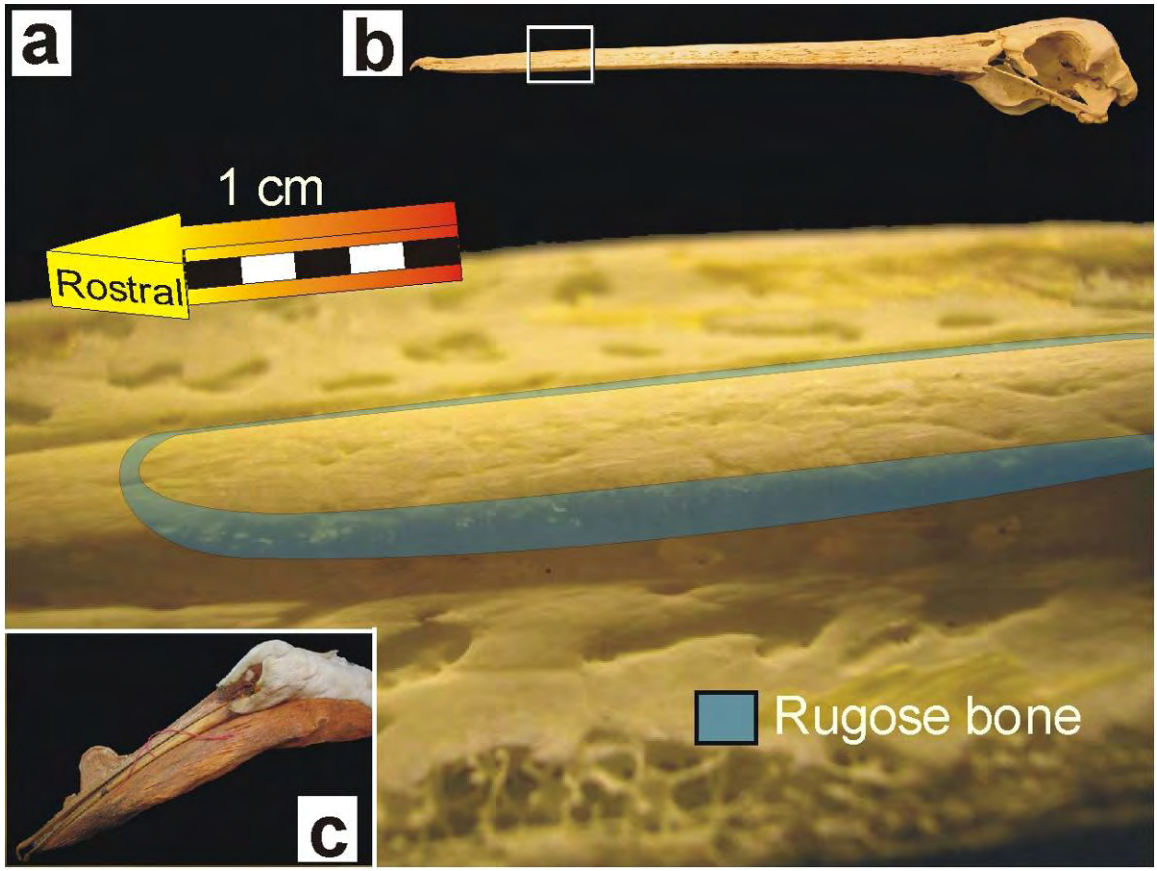

Figure A-9. Rugose bone on the premaxillae of the American white pelican *Pelecanus erythrorhynchos*. **a.** American white pelicans grow short crests of keratinous tissue for display in breeding that are shed at the end of the breeding season (May–July). Skeletal specimens from individuals that have died during this period show a faint annular rugosity at the location of the crest (ROM 151169). The annular rugosities of *P. erythrorhynchos* and *Sarkidiornis* are finer than the annular rugosities of extant rhinocerotids, most likely due to the difference in collagen fiber bundle size in metaplastically ossifying dermis. Nevertheless, the similarity in overall pattern, coupled with the similarity in skin elaborations in these taxa, suggests that annular rugosity provides a positive bony indicator for the presence of skin-derived horns and crests. **b.** Inset box shows the location of **a** on the skull. **c.** Study skin (ROM 34371) showing the size and location of the breeding crest.

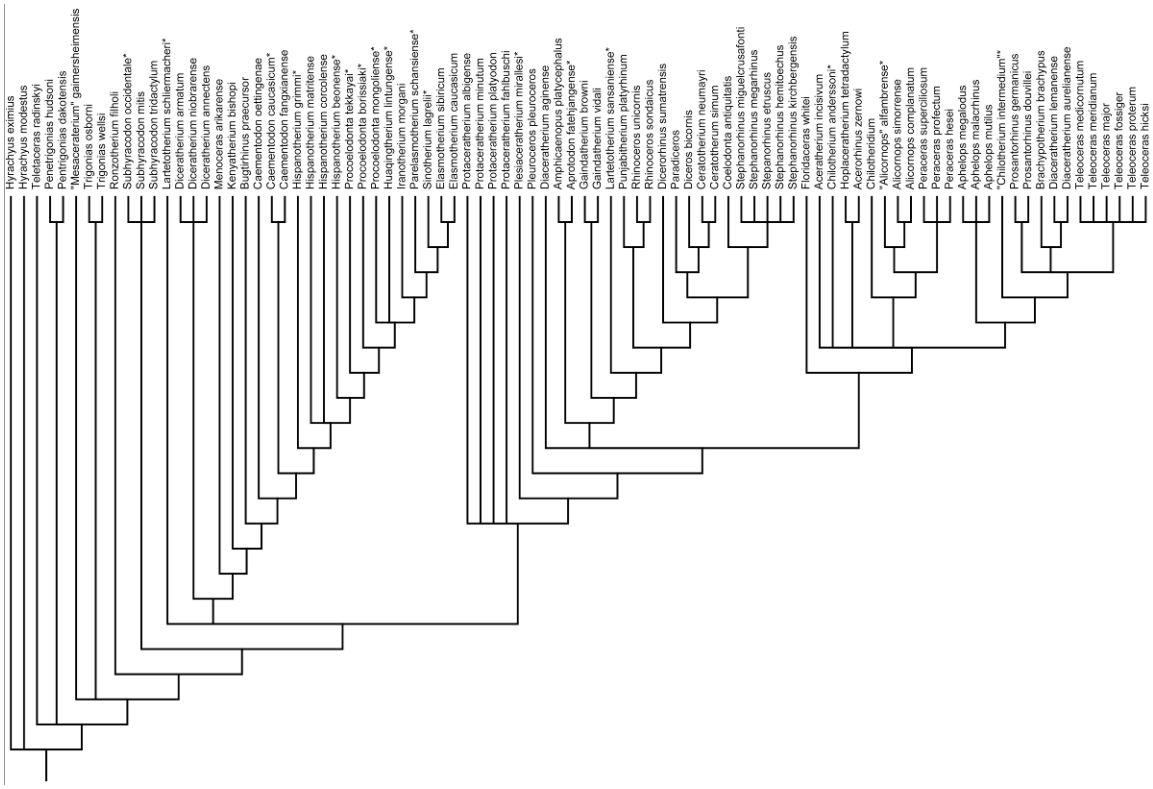

Figure A-10. Adams consensus supertree of extant and extinct Rhinocerotidae. Three morphologically based trees including extinct rhinocerotid taxa (Cerdeño 1995; Antoine 2002; Antoine et al. 2003) and three molecular trees of extant rhinocerotids (Morales and Melnick 1994; Tougard et al. 2001; Orlando et al. 2003) were coded using matrix representation with parsimony (MRP; Ragan 1992) in Mesquite 1.12 (Maddison and Maddison 2006). The tree matrix was then analyzed by a heuristic search in PAUP*4.10b (Swofford 2001). Analysis was stopped when the heuristic search returned 1000 equally parsimonious trees. The resulting trees were combined in an Adams consensus tree in PAUP*4.10b. Source code for MRP matrix, heuristic search trees, and other consensus trees are available from the authors by request.

Table A-1. Extant ingroup skeletal specimens. Institutional abbreviations: American Museum of Natural History (AMNH); Carnegie Museum of Natural History (CM); Muséum national d'Histoire naturelle (MNHN, MNHNA); Ohio University Vertebrate Collections (OUVC); United States National Museum of Natural History (USNM).

Specimen #	**Taxon**	**Common Name**
AMNH 90131	*Ceratotherium simum*	white rhinoceros
MNHN1928-310	*Ceratotherium simum*	white rhinoceros
MNHNA.2274	*Ceratotherium simum*	white rhinoceros
USNM 164598	*Ceratotherium simum*	white rhinoceros
AMNH 51854	*Ceratotherium simum*	white rhinoceros
OUVC 9541	*Ceratotherium simum*	white rhinoceros
AMNH 51855	*Ceratotherium simum cottoni*	northern white rhinoceros
AMNH 51856	*Ceratotherium simum cottoni*	northern white rhinoceros
AMNH 51857	*Ceratotherium simum cottoni*	northern white rhinoceros
AMNH 51858	*Ceratotherium simum cottoni*	northern white rhinoceros
AMNH 51859	*Ceratotherium simum cottoni*	northern white rhinoceros
AMNH 51860	*Ceratotherium simum cottoni*	northern white rhinoceros
AMNH 51861	*Ceratotherium simum cottoni*	northern white rhinoceros
AMNH 51862	*Ceratotherium simum cottoni*	northern white rhinoceros
AMNH 51864	*Ceratotherium simum cottoni*	northern white rhinoceros
AMNH 51865	*Ceratotherium simum cottoni*	northern white rhinoceros
AMNH 51870	*Ceratotherium simum cottoni*	northern white rhinoceros
AMNH 51872	*Ceratotherium simum cottoni*	northern white rhinoceros
AMNH 51881	*Ceratotherium simum cottoni*	northern white rhinoceros
AMNH 51882	*Ceratotherium simum cottoni*	northern white rhinoceros
AMNH 51883	*Ceratotherium simum cottoni*	northern white rhinoceros
AMNH 51889	*Ceratotherium simum cottoni*	northern white rhinoceros
AMNH 51890	*Ceratotherium simum cottoni*	northern white rhinoceros
AMNH 51891	*Ceratotherium simum cottoni*	northern white rhinoceros
AMNH 51897	*Ceratotherium simum cottoni*	northern white rhinoceros
AMNH 51912	*Ceratotherium simum cottoni*	northern white rhinoceros
AMNH 51913	*Ceratotherium simum cottoni*	northern white rhinoceros

AMNH 51917	*Ceratotherium simum cottoni*	northern white rhinoceros
AMNH 54125	*Ceratotherium simum cottoni*	northern white rhinoceros
AMNH 81815	*Ceratotherium simum simum*	southern white rhinoceros
AMNH 81816	*Ceratotherium simum simum*	southern white rhinoceros
AMNH 173576	*Dicerorhinus sumatrensis*	Sumatran rhinoceros
AMNH 54763	*Dicerorhinus sumatrensis*	Sumatran rhinoceros
AMNH 81892	*Dicerorhinus sumatrensis*	Sumatran rhinoceros
MNHNA.7965	*Dicerorhinus sumatrensis*	Sumatran rhinoceros
USNM 19885	*Dicerorhinus sumatrensis*	Sumatran rhinoceros
USNM 199551	*Dicerorhinus sumatrensis*	Sumatran rhinoceros
USNM 49561	*Dicerorhinus sumatrensis*	Sumatran rhinoceros
AMNH 113776	*Diceros bicornis*	black rhinoceros
AMNH 113777	*Diceros bicornis*	black rhinoceros
AMNH 113778	*Diceros bicornis*	black rhinoceros
AMNH 120448	*Diceros bicornis*	black rhinoceros
AMNH 13692	*Diceros bicornis*	black rhinoceros
AMNH 13693	*Diceros bicornis*	black rhinoceros
AMNH 13694	*Diceros bicornis*	black rhinoceros
AMNH 14136	*Diceros bicornis*	black rhinoceros
AMNH 187802	*Diceros bicornis*	black rhinoceros
AMNH 245690	*Diceros bicornis*	black rhinoceros
AMNH 27756	*Diceros bicornis*	black rhinoceros
AMNH 277578	*Diceros bicornis*	black rhinoceros
AMNH 30055	*Diceros bicornis*	black rhinoceros
AMNH 35740	*Diceros bicornis*	black rhinoceros
AMNH 54034	*Diceros bicornis*	black rhinoceros
AMNH 54283	*Diceros bicornis*	black rhinoceros
AMNH 54284	*Diceros bicornis*	black rhinoceros
AMNH 54383	*Diceros bicornis*	black rhinoceros
AMNH 80210	*Diceros bicornis*	black rhinoceros
AMNH 85174	*Diceros bicornis*	black rhinoceros

AMNH 85175	*Diceros bicornis*	black rhinoceros
AMNH 85176	*Diceros bicornis*	black rhinoceros
AMNH 85178	*Diceros bicornis*	black rhinoceros
AMNH 85179	*Diceros bicornis*	black rhinoceros
AMNH 85180	*Diceros bicornis*	black rhinoceros
AMNH 85181	*Diceros bicornis*	black rhinoceros
AMNH 85181[b]	*Diceros bicornis*	black rhinoceros
AMNH 85182	*Diceros bicornis*	black rhinoceros
AMNH 90204	*Diceros bicornis*	black rhinoceros
CM 1763	*Diceros bicornis*	black rhinoceros
CM 40561	*Diceros bicornis*	black rhinoceros
MNHN1931-581	*Diceros bicornis*	black rhinoceros
MNHN1944-278	*Diceros bicornis*	black rhinoceros
MNHN1974-124	*Diceros bicornis*	black rhinoceros
AMNH 34741	*Diceros bicornis somaliensis*	black rhinoceros
AMNH 34742	*Diceros bicornis somaliensis*	black rhinoceros
AMNH 202594	*Diceros* sp.	black rhinoceros
AMNH 204214	*Equus caballus*	domestic horse
AMNH 14096	*Equus quagga burchelli*	common zebra
AMNH 146717	*Rhinoceros sondaicus*	Javan rhinoceros
AMNH 146718	*Rhinoceros sondaicus*	Javan rhinoceros
AMNH 43	*Rhinoceros sondaicus*	Javan rhinoceros
MNHN1932-48	*Rhinoceros sondaicus*	Javan rhinoceros
MNHN1932-42	*Rhinoceros sondaicus*	Javan rhinoceros
MNHN1940-483	*Rhinoceros sondaicus*	Javan rhinoceros
MNHNA.2277	*Rhinoceros sondaicus*	Javan rhinoceros
MNHNA.7966	*Rhinoceros sondaicus*	Javan rhinoceros
MNHNA.7970B	*Rhinoceros sondaicus*	Javan rhinoceros
MNHNA.7971	*Rhinoceros sondaicus*	Javan rhinoceros
USNM 156507	*Rhinoceros sondaicus*	Javan rhinoceros
USNM 269392	*Rhinoceros sondaicus*	Javan rhinoceros

AMNH 119475	*Rhinoceros unicornis*	Indian rhinoceros
AMNH 171290	*Rhinoceros unicornis*	Indian rhinoceros
AMNH 245543	*Rhinoceros unicornis*	Indian rhinoceros
AMNH 274636	*Rhinoceros unicornis*	Indian rhinoceros
AMNH 35759	*Rhinoceros unicornis*	Indian rhinoceros
AMNH 54454	*Rhinoceros unicornis*	Indian rhinoceros
AMNH 54455	*Rhinoceros unicornis*	Indian rhinoceros
AMNH 54456	*Rhinoceros unicornis*	Indian rhinoceros
AMNH 70445	*Rhinoceros unicornis*	Indian rhinoceros
MNHN1932-49	*Rhinoceros unicornis*	Indian rhinoceros
MNHN1960-59	*Rhinoceros unicornis*	Indian rhinoceros
USNM 336953	*Rhinoceros unicornis*	Indian rhinoceros
USNM 398417	*Rhinoceros unicornis*	Indian rhinoceros
USNM 464963	*Rhinoceros unicornis*	Indian rhinoceros
USNM 540042	*Rhinoceros unicornis*	Indian rhinoceros
USNM 545847	*Rhinoceros unicornis*	Indian rhinoceros
USNM 545848	*Rhinoceros unicornis*	Indian rhinoceros
MNHNA.12.344	*Tapirus bairdii*	Baird's tapir
MNHN1906-550	*Tapirus indicus*	Asian tapir
MNHN1944-267	*Tapirus indicus*	Asian tapir
MNHN1982-034	*Tapirus pinchaque*	mountain tapir
MNHN1939-225	*Tapirus terrestris*	Brazilian tapir

Table A-2. Outgroup comparison specimens. Institutional abbreviations: American Museum of Natural History (AMNH); Carnegie Museum of Natural History (CM); Museum of the Rockies (MOR OST); Muséum national d'Histoire naturelle (MNHN, MNHNAE); Ohio University Vertebrate Collections (OUVC); Royal Ontario Museum (ROM); Senckenberg Museum (SMF); United States National Museum of Natural History (USNM); University of Michigan Museum of Zoology (UMMZ).

Specimen #	Taxon	Common Name
CM1557	*Antilocapra americana*	pronghorn
MNHNAE.685	*Cephalophus dorsalis*	bay duiker
MNHNAE.710	*Cephalophus* sp.	duiker
MOR OST 320	*Choloepus* sp.	two-toed sloth
AMNH 27675	*Giraffa camelopardalis*	giraffe
AMNH 81820	*Giraffa camelopardalis*	giraffe
AMNH 82001	*Giraffa camelopardalis*	giraffe
CM 5834	*Giraffa camelopardalis*	giraffe
CM10445	*Giraffa camelopardalis*	giraffe
CM2071	*Giraffa camelopardalis*	giraffe
CM2112	*Giraffa camelopardalis*	giraffe
CM30461	*Giraffa camelopardalis*	giraffe
CM59645 DC1559	*Giraffa camelopardalis*	giraffe
MNHNAE.806	*Giraffa camelopardalis*	giraffe
USNM 270902	*Hexaprotodon liberiensis*	pygmy hippopotamus
USNM 302054	*Hexaprotodon liberiensis*	pygmy hippopotamus
USNM 314046	*Hexaprotodon liberiensis*	pygmy hippopotamus
USNM 477361	*Hexaprotodon liberiensis*	pygmy hippopotamus
USNM 538815	*Hexaprotodon liberiensis*	pygmy hippopotamus
USNM 549277	*Hexaprotodon liberiensis*	pygmy hippopotamus
CM 1757	*Hippopotamus amphibius*	hippopotamus
CM 2033	*Hippopotamus amphibius*	hippopotamus
MNHN1943-27	*Hippopotamus amphibius*	hippopotamus
MNHN1944-999	*Hippopotamus amphibius*	hippopotamus
MNHN1959-131	*Hippopotamus amphibius*	hippopotamus

USNM 313712	*Hippopotamus amphibius*	hippopotamus
USNM 336648	*Hippopotamus amphibius*	hippopotamus
USNM 3883	*Hippopotamus amphibius*	hippopotamus
USNM 178701	*Hippopotamus amphibius amphibius*	hippopotamus
USNM 268091	*Hippopotamus amphibius amphibius*	hippopotamus
USNM 123387	*Hippopotamus amphibius capensis*	hippopotamus
USNM 36871	*Hippopotamus amphibius capensis*	hippopotamus
USNM 3882	*Hippopotamus amphibius capensis*	hippopotamus
USNM 162981	*Hippopotamus amphibius kiboko*	hippopotamus
USNM 182395	*Hippopotamus amphibius kiboko*	hippopotamus
USNM 182396	*Hippopotamus amphibius kiboko*	hippopotamus
USNM 182397	*Hippopotamus amphibius kiboko*	hippopotamus
USNM 254978	*Hippopotamus amphibius kiboko*	hippopotamus
USNM 161942	*Hippopotamus amphibius kiboko*	hippopotamus
USNM 162980	*Hippopotamus amphibius kiboko*	hippopotamus
CM 20960	*Hylochoerus meinertzhageni*	giant forest hog
CM 57916	*Hylochoerus meinertzhageni*	giant forest hog
USNM 163250	*Hylochoerus meinertzhageni*	giant forest hog
USNM 164627	*Hylochoerus meinertzhageni*	giant forest hog
USNM 308851	*Hylochoerus meinertzhageni*	giant forest hog
USNM 270155	*Hyemoschus aquaticus*	water chevrotain
USNM 482001	*Hyemoschus aquaticus*	water chevrotain
MNHNAE.696	*Madoqua* sp.	dik-dik
MNHNAE.676	*Neotragus pygmaeus*	royal antelope
AMNH 51200	*Okapia johnstoni*	okapi
MNHN159-262	*Okapia johnstoni*	okapi
MNHN1961-131	*Okapia johnstoni*	okapi
MNHN1996-102	*Okapia johnstoni*	okapi
USNM 308877	*Okapia johnstoni*	okapi
USNM 399337	*Okapia johnstoni*	okapi
CM20947	*Ovibos moschatus*	musk-ox

CM20955	*Ovibos moschatus*	musk-ox
CM21047	*Ovibos moschatus*	musk-ox
ROM CN 1148	*Ovibos moschatus*	musk-ox
CM 5154	*Potamochoerus porcus*	red river hog
USNM 164542	*Potamochoerus porcus*	red river hog
USNM 259174	*Potamochoerus porcus*	red river hog
MNHNAE.682	*Sylvicapra grimmae*	gray duiker
MNHN1927-18	*Tetracerus quadricornis*	chousingha
MNHN1983-122	*Tetracerus quadricornis*	chousingha
MNHN1995-148	*Tetracerus quadricornis*	chousingha
MNHN2004-295	*Tetracerus quadricornis*	chousingha
USNM 49692	*Tragulus napu*	greater Oriental chevrotain
USNM 578462	*Tragulus napu*	greater Oriental chevrotain
USNM 151800	*Tragulus napu borneanus*	greater Oriental chevrotain
USNM 151801	*Tragulus napu borneanus*	greater Oriental chevrotain
USNM 49772	*Tragulus napu borneanus*	greater Oriental chevrotain
USNM 49871	*Tragulus napu napu*	greater Oriental chevrotain
USNM 267335	*Tragulus napu perflavus*	greater Oriental chevrotain
USNM 49605	*Tragulus napu pretiosus*	greater Oriental chevrotain
UMMZ 152361	*Anhima cornuta*	horned screamer
ROM 91698	*Caloenas nicobarica*	Nicobar pigeon
ROM 126617	*Caloenas nicobarica*	Nicobar pigeon
CM 8126	*Cerorhinca monocerata*	rhinoceros auklet
CM 8125	*Cerorhinca monocerata*	rhinoceros auklet
CM 5119	*Cerorhinca monocerata*	rhinoceros auklet
ROM 39934	*Cerorhinca monocerata*	rhinoceros auklet
UMMZ 156989	*Chauna torquata*	crested screamer
UMMZ 149033	*Cyclura cornuta*	horned ground iguana
UMMZ 174428	*Cyclura cornuta*	horned ground iguana
UMMZ 128581	*Cyclura cornuta*	horned ground iguana
UMMZ 149036	*Cyclura ricordi*	Ricord's iguana

UMMZ 149096	*Iguana iguana*	green iguana
UMMZ 149093	*Iguana iguana*	green iguana
UMMZ 128103	*Iguana iguana*	green iguana
UMMZ 45409	*Iguana iguana*	green iguana
UMMZ 210529	*Moloch horridus*	thorny devil
ROM 0151169	*Pelecanus erythrorhynchos*	American white pelican
ROM 123578	*Pelecanus erythrorhynchos*	American white pelican
ROM 159651	*Pelecanus erythrorhynchos*	American white pelican
ROM 159650	*Pelecanus erythrorhynchos*	American white pelican
ROM 159653	*Pelecanus erythrorhynchos*	American white pelican
ROM 159652	*Pelecanus erythrorhynchos*	American white pelican
ROM 159649	*Pelecanus erythrorhynchos*	American white pelican
SMF2099	*Pelecanus occidentalis*	brown pelican
SMF2098	*Pelecanus occidentalis*	brown pelican
ROM 120525	*Sarkidiornis melanotos*	comb duck

Table A-3. Extinct ingroup fossil specimens. Institutional abbreviations: American Museum of Natural History Fossil Mammals Collection (AMNH FM); United States National Museum of Natural History (USNM); University of California Museum of Paleontology (UCMP).

Specimen #	Taxon	Age
AMNH FM 26091	*Amynodontopsis* sp. *("large sp.")*	E. "Sannoisan"
AMNH FM 21599	*Amynodontopsis* sp. *("small sp.")*	E. Oligocene
AMNH FM 104189	*Aphelops* cf. *Aphelops malacorhinus*	E. Hemphillian
AMNH FM Hig 29-436	*Aphelops* sp.	E. Hemphillian
UCMP 21802	*Ceratotherium neumayri*	Tortonian
AMNH FM 26342	*Chilotherium anderssoni*	E. Turolian
AMNH FM 26338	*Chilotherium habereri var laticeps*	-
AMNH China 30-L289	*Chilotherium sp.*	E. Turolian
AMNH China 46-387	*Chilotherium sp.*	E. Turolian
AMNH China 80-L619	*Chilotherium sp.*	E. Turolian
AMNH FM 7324	*Diceratherium annectens*	Oligocene
AMNH FM 112176	*Diceratherium armatum*	E. Lt Arikareean
USNM 11682	*Diceratherium armatum*	Arikareean
AMNH FM 112171	*Diceratherium sp.*	E. Arikareean?
AMNH FM 111948	*Diceratherium sp.*	E. Barstovian
AMNH FM 112185	*Diceratherium sp.*	E. Arikareean
AMNH FM 112187	*Diceratherium sp.*	E. Lt Arikareean
AMNH FM 112195	*Diceratherium sp.*	E. Lt Arikareean
AMNH FM 26660	*Forstercooperia confluens*	M. "Bartonian"
AMNH FM 26643	*Forstercooperia sp.*	M. "Bartonian"
AMNH FM 26531	*Huaqingtherium lintungense*	Lt. Vindobonian
AMNH FM 26521	*Huaqingtherium lintungense*	Lt. Vindobonian
AMNH FM 12364	*Hyrachyus eximius*	Bridgerian
AMNH FM 13756	*Hyrachyus modestus*	Bridgerian
AMNH FM 12296	*Hyracodon nebraskensis*	
AMNH FM 14229	*Menoceras arikarense*	Late Arikareean
AMNH FM 22458	*Menoceras arikarense*	Late Arikareean

AMNH FM 26892	*Menoceras arikarense*	Late Arikareean
AMNH FM 39358	*Menoceras arikarense*	-
AMNH FM 86114	*Menoceras arikarense*	Late Arikareean
AMNH FM 86115	*Menoceras arikarense*	Late Arikareean
AMNH FM 86116	*Menoceras arikarense*	Late Arikareean
AMNH FM 86223	*Menoceras arikarense*	Late Arikareean
AMNH FM 86227	*Menoceras arikarense*	Late Arikareean
AMNH FM 86229	*Menoceras arikarense*	Late Arikareean
AMNH FM 112245	*Menoceras arikarense*	Late Arikareean
USNM 10297	*Menoceras arikarense*	Arikareean
AMNH FM 82849	*Menoceras barbouri*	E. Hemingfordian
AMNH FM 112246	*Menoceras sp.*	Lt. Lt Arikareean
AMNH FM 112250	*Menoceras sp.*	Lt. Lt Arikareean
AMNH FM 1496	*Metamynodon planifrons*	E. Orellan
AMNH FM 547	*Metamynodon planifrons*	-
AMNH FM 114923	*Peraceras hesei*	Lt. Lt. Barstovian
AMNH FM 19185	*Procoelodonta mongoliense*	E. ? Vindobonian
AMNH FM 21601	*Sharamynodon mongoliensis*	M. "Ludian"
AMNH 8088	*Subhyracodon sp.*	E. Whitneyan
AMNH FM 1126	*Subhyracodon sp.*	M. Whitneyan
AMNH FM 1127	*Subhyracodon sp.*	M. Whitneyan
AMNH FM 541	*Subhyracodon sp.*	M. Whitneyan
AMNH FM Lusk 0-151-4114	*Subhyracodon sp.*	Chadronian/Orellan
AMNH FM 109618	*Teleoceras* cf. *Teleoceras minor*	E. E. Valentinian
USNM Fla. 147-2452	*Teleoceras proterum*	E. Hemphillian
USNM Fla. 29-522	*Teleoceras proterum*	E. Hemphillian
AMNH FM 115853	*Teleoceras sp.*	E. Hemphillian
AMNH FM 8404	*Teleoceras sp.*	Clar. - Hemp.
UCMP 129000	*Teletaceras radinskyi*	
AMNH FM 12389	*Trigonias osborni*	E. Chadronian

AMNH B.H. 12-512	*Trigonias wellsi*	M. Chadronian
AMNH FM 26034	*Zaisamynodon borizovi*	E. "Sannoisan"

Literature Cited

Antoine P-O 2002. *Phylogénie et évolution des Elasmotheriina (Mammalia, Rhinocerotidae.)* Paris: Publications scientifiques du Muséum.

Antoine P-O, Duranthon F, Wellcome J-L. 2003. *Alicornops* (Mammalia, Rhinocerotidae) dans le Miocene superieur des Collines Bugti (Balouchistan, Pakistan): implications phylogenetiques. GEODIVERSITAS 25:575–603.

Benjamin M, Kumai T, Milz S, Boszczyk BM, Boszczyk AA, Ralphs JR. 2002. The skeletal attachment of tendons—tendon 'entheses'. Comparative Biochemistry and Physiology Part A 133:931–945.

Cerdeño E. 1995. Cladistic analysis of the family Rhinocerotidae (Perissodactyla). American Museum Novitates 3143:1–25.

Haines RW, Mohuiddin A. 1968. Metaplastic bone. Journal of Anatomy 103:96–98.

Hieronymus TL, Witmer LM, Ridgely RC. 2006. Structure of white rhinoceros (*Ceratotherium simum*) horn investigated by X-ray computed tomography and histology with implications for growth and external form. Journal of Morphology 267:1172–1176.

Kingdon J. 1979. East African mammals: An atlas of evolution in Africa. Vol.3. Part B, Large mammals London: Academic Press.

Maddison WP, Maddison DR. 2006. Mesquite: a modular system for evolutionary analysis, v1.12 (http://mesquiteproject.org).

Morales JC, Melnick DJ. 1994. Molecular systematics of the living rhinoceros. Molecular Phylogenetics and Evolution 3:128–134.

Orlando L, Leonard JA, Thenot A, Laudet V, Guerin C, Hänni C. 2003. Ancient DNA analysis reveals woolly rhino evolutionary relationships. Molecular Phylogenetics and Evolution 28:485–499.

Ragan MA. 1992. Phylogenetic inference based on matrix representation of trees. Molecular Phylogenetics and Evolution 1:53–58.

Ryder ML. 1962. Structure of rhinoceros horn. Nature 193:1199–1201.

Schumacher Sv. 1931. Integument der Mammalier. In: Bolk L, Goppert E, Kallius E, Lubosch W, editors. Handbuch der Vergleichenden Anatomie der Wirbeltiere. Berlin: Urban und Schwarzenburg. p. 449–504.

Shadwick RE, Russell AP, Lauff RF. 1992. The structure and mechanical design of rhinoceros dermal armour. Philosophical Transactions of the Royal Society of London. Series B, Biological sciences 337:419–428.

Sokolov VE. 1982. Mammal skin. Berkeley: University of California Press.

Swofford DL. 2001. PAUP*: phylogenetic analysis using parsimony (*and other methods), v4.10b. Sunderland: Sinauer Associates.

Tougard C, Delefosse T, Hänni C, Montelgard C. 2001. Phylogenetic relationships of the five extant rhinoceros species (Rhinocerotidae, Perissodactyla) based on mitochondrial cytochrome b and 12S rRNA genes. Molecular Phylogenetics & Evolution 19:34–44.

APPENDIX B: SUPPLEMENTARY INFORMATION FOR CHAPTER 3

Table B-1. Character scores for taxa by region. Ros: rostral; Int: internasal; Nas: nasal; Lor: loreal; Pre: prefrontal; Spl: supralabial; Fro: frontal; Par: parietal; Squ: squamosal; Tem: temporal; Spo: Supraocular; Sym: symphyseal; Inf: infralabial; Sub: sublabial; Gul: gular. Character codes: 0: single plate or scale; 1: plate or scale continuous with adjacent region; 2: multiple irregular scales; 3: multiple hexagonal scales; 4: scaleless soft skin; 5: feathered skin. Figure 9 shows the phylogenetic hypothesis used for this study.

Taxon	Ros	Int	Nas	Lor	Pre	Spl	Fro	Par	Squ	Tem	Spo	Sym	Inf	Sub	Gul
Basiliscus basiliscus	0	3	0	3	3	2	3	3	3	3	3	0	2	3	3
Basiliscus vittatus	0	3	0	3	3	2	3	3	3	3	3	0	2	3	3
Chamaeleo calyptratus	3	3	2	3	3	3	3	3	3	3	3	3	3	3	3
Chamaeleo jacksoni	3	3	2	3	3	3	3	3	3	3	3	3	3	3	3
Chlamydosaurus kingii	2	3	2	3	3	3	3	3	3	3	3	2	3	3	3
Cordylus giganteus	0	0	0	2	0	2	0	2	3	3	2	0	2	2	3
Corytophanes cristatus	0	3	0	3	3	2	3	3	3	3	3	0	2	3	3
Cyclura cornuta	0	2	0	3	3	2	3	3	3	3	3	0	2	2	3
Cyclura ricordi	0	3	0	3	3	2	3	3	3	3	3	0	2	3	3
Elgaria multicarinata	0	2	0	2	2	2	0	3	3	3	2	0	2	2	2
Enyalioides laticeps	2	3	2	3	3	2	3	3	3	3	3	2	2	3	3
Gekko gecko	0	3	2	3	3	2	3	3	3	3	3	0	2	3	3
Gerrhonotus liocephalus	0	2	0	2	2	2	0	3	3	3	2	0	2	2	2
Gerrhosaurus major	0	0	0	2	0	2	0	2	2	3	2	0	2	2	2
Heloderma horridum	0	3	2	3	3	2	3	3	3	3	3	0	2	3	?
Hemitheconyx caudicinctus	0	3	2	3	3	3	3	3	3	3	3	0	3	3	3
Iguana iguana	0	3	0	2	2	2	2	3	3	3	3	0	2	2	2
Laemanctus serratus	0	3	0	3	3	2	3	3	3	3	3	?	2	3	3
Lamprolepis smaragdina	0	0	2	2	0	2	0	2	2	3	2	0	2	2	?
Lepidophyma flavimaculatus	0	2	2	2	2	2	0	2	2	2	0	0	1	1	?
Moloch horridus	3	3	2	3	3	3	3	3	3	3	3	3	3	3	3
Oplurus cuvieri	0	3	2	3	2	2	2	3	3	3	3	2	2	3	3
Phrynosoma cornuta	2	3	2	2	3	3	3	3	2	3	3	2	3	2	3
Sceloporus poinsetti	0	3	2	2	2	2	2	2	2	3	2	0	2	2	3
Tiliqua rugosa	0	0	0	2	0	2	2	2	3	3	2	0	2	2	?
Tiliqua scincoides	0	0	0	2	0	2	2	2	3	3	2	0	2	2	3
Uromastyx aegypticus	2	3	2	3	3	3	3	3	3	3	3	3	3	3	3
Varanus beccari	3	3	3	3	3	3	3	3	3	3	3	3	3	3	3
Varanus exanthematicus	2	3	3	3	3	3	3	3	3	3	3	2	3	3	3
Sphenodon punctatus	2	3	3	3	3	2	3	3	3	3	3	3	2	3	3
cf. *Geochelone*	0	2	2	1	0	1	0	?	?	?	3	1	1	2	3
Chelonia mydas	1	2	1	1	2	1	2	2	2	2	2	1	1	?	?
Chelydra serpentina	1	2	2	1	2	1	2	2	2	3	2	1	1	1	3
Malaclemys terrapin	1	4	1	1	4	1	4	1	1	4	4	1	1	?	?
Sternotherus minor	1	4	4	1	4	1	4	4	4	4	?	1	1	1	?
Alligator mississippiensis	2	2	2	3	2	3	1	1	2	3	0	3	3	3	3
Crocodylus novaeguiniae	2	2	2	2	2	3	1	1	2	2	1	3	3	3	3
Crocodylus porosus	2	2	2	2	2	2	1	1	2	2	0	2	2	0	3

Aceros undulatus	1	0	1	1	5	1	5	5	5	5	5	1	1	1	4
Alca torda	0	5	0	5	5	0	5	5	5	5	5	1	1	5	5
Anas clypeata	0	4	4	4	5	0	5	5	5	5	5	0	4	4	4
Andigena laminirostris	1	1	5	4	5	0	5	5	5	5	5	1	1	1	5
Anseranas semipalmata	0	0	4	4	4	0	5	5	5	5	5	0	0	4	4
Apteryx australis mantelli	0	1	1	5	5	0	5	5	5	5	5	0	1	1	?
Buceros vigil	1	2	5	1	5	1	5	5	5	5	5	1	1	1	4
Bucorvus abyssinicus	0	0	5	4	5	0	5	5	5	5	5	1	1	1	4
Buteo jamaicensis	1	1	1	5	5	1	5	5	5	5	5	1	1	5	5
Butorides striatus	1	1	0	4	5	1	5	5	5	5	5	1	1	1	5
Bycanistes brevis	1	0	1	1	5	1	5	5	5	5	5	1	1	1	4
Caloenas nicobarica	0	4	4	5	5	4	5	5	5	5	5	0	4	4	5
Calonectris diomedea	1	1	0	5	5	0	5	5	5	5	5	0	0	0	?
Casuarius casuarius	0	0	4	4	1	0	1	4	4	4	5	0	0	0	4
Catharacta skua	1	0	1	5	5	1	5	5	5	5	5	1	1	1	?
Cepphus grylle	1	5	1	5	5	1	5	5	5	5	5	1	1	?	1
Cerorhinca monocerata	0	1	1	5	5	0	5	5	5	5	5	1	1	5	5
Colaptes auratus	1	1	1	5	5	1	5	5	5	5	5	1	1	1	5
Corvus brachyrhynchos	1	1	5	5	5	1	5	5	5	5	5	1	1	1	5
Crax alector	1	4	4	4	5	1	5	5	5	5	5	0	0	0	5
Crax rubra	0	4	4	5	5	0	5	5	5	5	5	0	4	4	?
Cygnus buccinator	0	4	4	4	5	0	5	5	5	5	5	0	4	4	4
Cygnus olor	0	4	4	4	4	0	5	5	5	5	5	0	0	4	5
Dromaius novaehollandiae	0	0	4	4	5	0	5	5	5	4	5	0	0	0	5
Eudyptes chrysolophus	1	1	5	5	5	0	5	5	5	5	5	1	1	5	5
Fratercula arctica	0	0	0	5	5	0	5	5	5	5	0	0	1	1	1
Fratercula corniculata	0	0	0	5	5	0	5	5	5	5	5	0	1	1	1
Gallinula chloropus	1	1	1	0	1	1	5	5	5	5	5	1	1	1	5
Gavia immer	1	1	0	5	5	1	5	5	5	5	5	1	1	1	5
Lanius excubitor	1	1	1	5	5	1	5	5	5	5	5	1	1	1	?
Larus delewarensis	1	1	1	5	5	1	5	5	5	5	5	1	1	1	5
Macronectes giganteus	0	0	0	5	5	0	5	5	5	5	5	0	0	0	?
Malacorhynchos membranaceus	0	4	4	5	5	0	5	5	5	5	5	0	0	4	4
Mitu mitu	1	1	4	5	5	1	5	5	5	5	5	1	1	5	5
Oreophasis derbianus	1	5	5	5	5	1	4	5	5	5	4	1	1	5	5
Otus asio	1	1	1	5	5	1	5	5	5	5	5	1	1	5	5
Pelecanus erythrorhynchos	0	0	1	4	5	0	5	5	5	5	5	0	1	1	4
Phalacrocorax auritus	0	0	-	5	5	0	5	5	5	5	5	0	1	1	4
Phoebastria immutabilis	0	0	0	5	5	0	5	5	5	5	5	0	1	1	5
Pterodroma incerta	1	1	0	5	5	0	5	5	5	5	5	0	0	0	?
Pygoscelis adeliae	1	1	1	0	5	0	5	5	5	5	5	1	1	1	5
Sarkidiornis melanotos	0	4	4	5	5	0	5	5	5	5	5	0	0	4	4
Somateria mollissima	1	1	4	5	4	0	5	5	5	5	5	0	0	4	?
Struthio camelus	0	4	4	5	5	0	5	5	5	5	5	0	1	1	5
Sula bassana	0	0	-	4	5	0	5	5	5	5	5	0	1	1	4

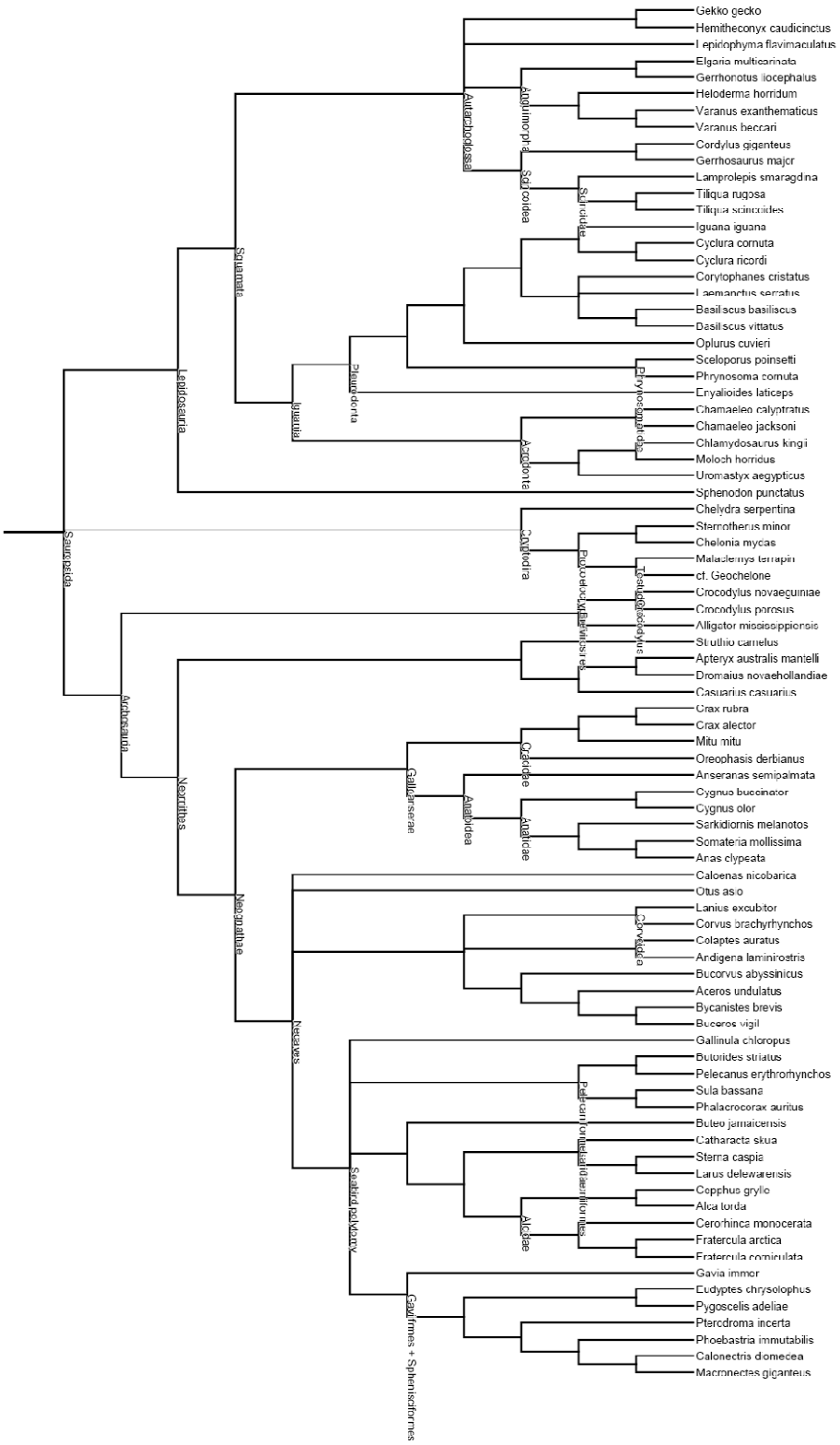

Figure B-1. Composite phylogenetic tree of Sauropsida used in this study.

APPENDIX C: SUPPLEMENTARY INFORMATION FOR CHAPTER 4

Table C-1. Taxa included in this study. Taxa in bold were included in ancestral character state reconstructions. Material examined is coded as: O, osteological material; S, study skin (whole or partial preservation); P, verification in Calphotos archive for partial study skins; F, fresh, frozen, or formalin-fixed; µCT, MicroCT scanned; VI, MicroCT with vascular injection; H, histological preparation of rhamphotheca.

Taxon	**Material examined**
Aceros undulatus	O, S, P
Aethia cristatella	S
Alca torda	O, S
Anas clypeata	O, F, VI
Anastomus lamelligerus	O, S
Andigena laminirostris	S
Anhima cornuta	O
Anhinga melanogaster	O
Anseranas semipalmata	O, S
Anthracoceros malabaricus	O
Aptenodytes forsteri	O
Apteryx australis	O, S
Apteryx owenii	O
Aramus guarana	O
Ardea cinerea	O
Ardeotis kori	O
Argusianus argus	O

Balaeniceps rex	O
Buceros bicornis	O
Buceros hydrocorax	O
Buceros vigil	O, S
Bucorvus abyssinicus	O, S
Bucorvus leadbetteri	O
Buteo jamaicensis	O, F, µCT
Butorides striatus	O, F, µCT
Bycanistes brevis	O, S, P
Bycanistes bucinator	O
Caloenas nicobarica	O, S
Calonectris diomedea	O, S, P
Casuarius casuarius	O, S
Casuarius unappendiculatus	O, S, P
Catharacta skua	O, S, P
Cepphus grylle	O
Ceratogymna fistulator	O
Cerorhinca monocerata	O, S
Chauna torquata	O, S, P
Chionis alba	O
Colaptes auratus	O, F, VI, H
Corvus brachyrhynchos	O, F, VI, H

Crax alector	O, S
Crax rubra	O, S
Cygnus buccinator	O, F
Cygnus olor	O, S
Daption capense	O
Didunculus strigirostris	S
Diomedea antipodensis	O
Diomedea melanophrys	O
Dromaius novaehollandiae	O, F
Dryocopus pileatus	O
Egretta garzeta	O
Eudyptes chrysolophus	O, S
Eudyptula minor	O
Eurypyga helias	O
Falco rusticolus	O
Fratercula arctica	O, S
Fratercula cirrhata	O, S
Fratercula corniculata	O, S
Fregata minor	O
Fregata sp.	O
Fulmarus glacialis	O
Gallinula chloropus	O, F, µCT

Gavia immer	O, F, VI
Gavia stellata	O
Halobaena caerulea	O
Lanius excubitor	O, S, P
Larus argentatus	O
Larus delewarensis	O, F, VI, H
Macronectes giganteus	O, S, P
Macronectes sp.	O
Malacorhynchus membranaceus	O
Mergus cucullatus	O
Mergus merganser	O
Mitu mitu	S
Nyctibius grandis	O
Oceanites oceanicus	O
Oreophasis derbianus	S
Otus asio	O, F, VI, H
Pachyptila desolata	O
Pachyptila turtur	O
Pachyptila vittata	O
Pelecanoides urinatrix	O
Pelecanus erythrorhynchos	O, S, F
Pelecanus onocrotalus	O

Penelopides panini	O
Phaethon lepturus	O
Phalacrocorax aristotelis	O
Phalacrocorax auritus	O, F, VI, H
Phalacrocorax carbo	O
Phobastria immutabilis	O, F, µCT
Pinguinus impinnis	O
Podiceps cristatus	O
Psophia leucoptera	O
Pterodroma hypoleuca	O
Pterodroma incerta	O, S, P
Pteroglossus aracan	O
Pygoscelis adeliae	O, S, P
Rhynchops flavirostris	O
Rhynchops niger	O
Rhynchotus rufescens	O
Sarkidiornis melanotos	O, S
Somateria mollissima	O, S
Somateria spectabilis	O
Spheniscus humboldti	O
Sterna caspia	O
Struthio camelus	O

Sula bassana	O, F
Sula dactylatra	O
Tinamus major	O
Tockus erythrorhynchus	O
Tockus flavirostris	F, µCT
Turdus merula	O
Uria lomvia	O
Xema sabini	O

APPENDIX D: SUPPLEMENTARY INFORMATION FOR CHAPTER 5

List of centrosaurine specimens and outgroups examined for gross osteological correlates. Museum abbreviations: AMNH FR, American Museum of Natural History Fossil Reptiles; MOR, Museum of the Rockies; ROM, Royal Ontario Museum; TMP, Royal Tyrrell Museum of Palaeontology; UCMP, University of California Museum of Paleontology.

Achelousaurus horneri—MOR 485, MOR 571, MOR 591; *Anchiceratops ornatus*—ROM 802; *Anchiceratops* sp.—AMNH FR 5251; Centrosaurinae indet. —ROM 49862; *Centrosaurus apertus*—ROM 12776, ROM 767, TMP 1966.33.17; *Centrosaurus* sp.—ROM 831; cf. *Centrosaurus*—AMNH FR 5442, ROM 12782, ROM 12787, ROM 43214, ROM 49863, ROM 636, ROM 641, ROM 728, TMP 1992.36.224; *Centrosaurus* cf. *C. apertus*—TMP 1987.18.20, TMP 1989.18.148; *Chasmosaurus brevirostris*—ROM 839; *Einiosaurus procurvicornis*—MOR 373a, MOR 373b, MOR 373c, MOR 456a, MOR 456b, MOR 456c, MOR 456d, MOR 456e; *Pachyrhinosaurus* cf. *P. canadensis*—Drumheller skull[1], UCMP 88H8-4-4; *Pachyrhinosaurus lakustai*—TMP 1985.112.1, TMP 1985.112.28, TMP 1986.55.102, TMP 1986.55.155, TMP 1986.55.206, TMP 1986.55.258, TMP 1987.55.110, TMP 1987.55.156, TMP 1987.55.228, TMP 1987.55.304, TMP 1987.55.320, TMP 1987.55.323, TMP 1987.55.81, TMP 1989.55.1009, TMP 1989.55.1111, TMP 1989.55.1112, TMP 1989.55.1125, TMP 1989.55.1131, TMP 1989.55.1185, TMP 1989.55.1234, TMP 1989.55.1396, TMP 1989.55.1524, TMP 1989.55.172, TMP 1989.55.172, TMP 1989.55.188, TMP 1989.55.21, TMP 1989.55.203, TMP 1989.55.207, TMP 1989.55.256, TMP 1989.55.367,

TMP 1989.55.427, TMP 1989.55.467, TMP 1989.55.561, TMP 1989.55.566, TMP 1989.55.566, TMP 1989.55.72, TMP 1989.55.781, TMP 1989.55.918, TMP 1989.55.927; TMP 1989.55.931, TMP 1989.55.958; Protoceratops andrewsi—AMNH FR 6429.

[1]This specimen, described in Langston (1967), was studied from a cast housed in the collections of the Royal Tyrrell Museum of Palaeontology.

Table D-1. Extant histological specimens.

Taxon	**Specimen #**	**Location**	**Tissues sampled**
Colaptes auratus	OUVC 10400	premaxilla and rictus	Bone and soft tissue
Corvus brachyrhynchos	OUVC 10403	premaxilla and rictus	Bone and soft tissue
Gerrhosaurus major	OUVC 10410	premaxilla and maxilla	Bone and soft tissue
Hemitheconyx caudicinctus	OUVC 10411	premaxilla and maxilla	Bone and soft tissue
Larus delewarensis	OUVC 10399	premaxilla and rictus	Bone and soft tissue
Lepidophyma flavimaculatus	OUVC 10418	premaxilla and maxilla	Bone and soft tissue
Oplurus cuvieri	OUVC 10419	premaxilla and maxilla	Bone and soft tissue
Otus asio	OUVC 10402	maxillary rostrum	Bone and soft tissue
Phalacrocorax auritus	OUVC 10401	premaxilla and rictus	Bone and soft tissue
Varanus exanthematicus	OUVC 10414	premaxilla, maxilla, dentary	Bone and soft tissue
Ceratotherium simum	OUVC 9541	nasal horn, frontal horn	Bone and soft tissue
Giraffa camelopardalis	OUVC ?	median ossicone	Bone and soft tissue
Ovibos moschatus	UAM 86916	frontal horn boss	Bone and horn sheath
Crocodylus porosus	OUVC 10576	maxilla	Bone
Alligator mississippiensis	OUVC 9633	maxilla	Bone
Chrysemys picta	OUVC unnumbered	maxilla	Bone and horny beak

Table D-2. Paleohistological specimens.

Specimen #	Source specimen #	Description
TMP 1993.55.2	TMP 1989.55.894	Border of bony nostril
TMP 1993.55.8	TMP 1989.55.1038	Caudal nasal boss
TMP 1993.55.9	TMP 1989.55.894	Tip of developing nasal horn core
TMP 1993.55.10	TMP 1989.55.894	Lateral surface of developing nasal horn core
TMP 1993.55.11	TMP 1989.55.174	Lateral surface of developing nasal horn core
TMP 1993.55.12	TMP 1986.55.48	Lateral surface of developing nasal horn core
TMP 1993.55.13	TMP 1987.55.161	Lateral surface of developing nasal horn core
TMP 1993.55.16	TMP 1989.55.1342	Basal sulcus of nasal boss
TMP 1993.55.17	TMP 1989.55.1342	Lateral surface of nasal boss
TMP 1993.55.18	TMP 1989.55.1342	Lateral surface of nasal adjacent to boss
TMP 1993.55.20	TMP 1989.55.1342	Basal sulcus of nasal boss